Journal of Applied Engineering and Technological Science
Vol 7(1) 2025: 679-707

PREDICTING BENTONITE PLASTIC CONCRETE PERFORMANCE USING MACHINE LEARNING

Sameh Fuqaha[1], Ahmad Zaki[2*]
Master Program of Civil Engineering, Universitas Muhammadiyah Yogyakarta, Yogyakarta, 55183, Indonesia[12]
Department of Civil Engineering, Universitas Muhammadiyah Yogyakarta, 55183 Yogyakarta, Indonesia[2]
ahmad.zaki@umy.ac.id

Received: 31 May 2025, Revised: 08 October 2025, Accepted: 27 October 2025
**Corresponding Author*

ABSTRACT
This study develops an interpretable machine learning framework to predict the mechanical properties of bentonite plastic concrete (BPC), an essential material for low-permeability geotechnical structures. Traditional testing of BPC is time- and cost-intensive, while empirical equations often fail to capture the nonlinear effects of bentonite and curing conditions. To address these limitations, four ensemble learning models were optimized using the Forensic-Based Investigation Optimization (FBIO) algorithm, a parameter-free metaheuristic inspired by investigative search processes. The models were trained on three curated experimental datasets to predict slump, tensile strength, and elastic modules. Among all, XGB–FBIO achieved the highest accuracy for slump (R^2 = 0.98) and tensile strength (R^2 = 0.99), while GBRT–FBIO performed best for elastic modulus (R^2 = 0.97). SHapley Additive exPlanations (SHAP) analysis revealed curing time, cement, and water content as the most influential variables. The results demonstrate that the proposed framework can replace repetitive laboratory trials with data-driven insights, providing engineers with a reliable, explainable, and resource-efficient tool for optimizing BPC mix designs in environmental and geotechnical applications.
Keywords : *Bentonite Plastic Concrete (BPC), Ensemble Learning, Forensic-Based Investigation Optimization (FBIO), Mechanical Property Prediction, SHAP Analysis.*

1. Introduction

The management of industrial wastewater presents a significant challenge in the global sustainability agenda, particularly due to its high content of toxic heavy metals such as chromium (Cr), mercury (Hg), copper (Cu), lead (Pb), cadmium (Cd), zinc (Zn), and nickel (Ni) (Keramati et al., 2019). These contaminants are persistent, bio accumulative, and pose severe ecological risks due to their non-biodegradable nature. Among the various treatment strategies available, adsorption has gained prominence for its cost-effectiveness and efficiency in removing metal ions from aqueous environments (Liu et al., 2020). Natural clay minerals, especially bentonite, have attracted increasing attention due to their favorable physicochemical properties, including high surface area, strong ion exchange capacity, environmental safety, and widespread availability (Barakan & Aghazadeh, 2021).

Bentonite, primarily consisting of montmorillonite along with minor constituents such as calcite and quartz, has been extensively studied for heavy metal adsorption (Dhar et al., 2023; Shubber & Kebria, 2023). Recent advancements have explored the integration of bentonite into concrete matrices to form bentonite plastic concrete (BPC), a composite material that inherits the mechanical strength of conventional concrete and the low-permeability, self-sealing nature of bentonite. BPC is particularly suitable for geotechnical and environmental applications, such as cut-off walls in dam foundations, due to its viscoelasticity, hydraulic impermeability, and deformation tolerance (Bahrami & Mir Mohammad Hosseini, 2022). Abbaslou et al. (2016) illustrated the dual functionality of BPC in removing cadmium ions from water while also enhancing durability and reducing structural cracking.

Traditional experimental and empirical approaches used to evaluate the mechanical and durability properties of bentonite plastic concrete (BPC) are constrained by high cost, time consumption, and limited adaptability to diverse mix proportions and curing environments (Ni et al., 2025). The inherent variability in bentonite content, water-to-cement ratio, and curing

conditions introduces complex nonlinear interactions that conventional regression-based or empirical models fail to capture, leading to substantial uncertainty and inconsistent predictive accuracy (M. Zhang & Kang, 2025). These challenges hinder the efficient optimization of BPC mix designs and restrict its large-scale implementation in sustainable infrastructure projects. In contrast, machine learning (ML) offers a powerful, data-driven alternative capable of addressing these shortcomings by learning complex multivariate relationships from existing experimental data (A. Ullah et al., 2025).

ML techniques have gained remarkable traction in predicting the mechanical and durability properties of diverse material systems, including concrete, geopolymer binders, and composite materials (Darimolyo et al., 2025; Deng et al., 2024; Nurega et al., 2025; Rozzaq et al., 2025). Traditional empirical or regression-based models often struggle to capture the highly nonlinear and multivariate relationships between mix composition, curing conditions, and performance outputs, leading to suboptimal accuracy and limited generalization (Li et al., 2025). In contrast, modern ML algorithms such as Random Forest (RF), Gradient Boosting (GB), Support Vector Machines (SVM), and Artificial Neural Networks (ANN) have demonstrated superior capabilities in identifying complex correlations and interactions among input variables (Fuqaha, Nugroho, et al., 2025; Lal Mohiddin et al., 2025). These models have been widely applied to predict compressive strength, flexural strength, tensile strength, and durability indices, often achieving substantial error reduction compared to conventional statistical approaches (Gamil, 2023).

Recent studies have advanced the use of ML for concrete and composite materials, focusing on performance optimization and sustainability. For instance, ensemble and hybrid models have been developed to predict the strength of high-performance concretes and geopolymers by integrating microstructural and mix design features (Fuqaha et al., 2025; Kibrete et al., 2023). Similarly, deep learning and metaheuristic-optimized algorithms have been employed for damage detection, crack analysis, and mechanical performance forecasting of fiber-reinforced composites (Ramezani et al., 2025).

As infrastructure projects increasingly adopt bentonite plastic concrete (BPC) for sustainable and low-permeability applications, there is a growing need for intelligent, data-driven models capable of accurately predicting their mechanical behavior. Machine learning (ML) offers a transformative solution, enabling high-accuracy predictions using historical datasets without the need for repetitive and resource-intensive testing. This study aims to develop an optimized and interpretable ensemble learning (EL) framework integrated with forensic-based investigation optimization (FBIO) to forecast key mechanical properties of BPC. Beyond predictive accuracy, the proposed framework contributes to sustainable materials engineering by reducing experimental waste, optimizing material usage, and minimizing the carbon and resource footprint associated with conventional testing. Moreover, the integration of a user-friendly web application supports the digital transformation of construction practices, enabling engineers to make rapid, data-informed decisions that enhance efficiency, sustainability, and environmental remediation in infrastructure development.

2. Literature Review

Recent literature highlights three main directions in machine learning applications for concrete performance prediction: standalone models, ensemble learning approaches, and optimization-enhanced frameworks. The first category involves standalone ML algorithms such as artificial neural networks (ANN), multivariate adaptive regression splines (MARS), and M5 Tree regression (Abbaslou et al., 2016; Alidoust et al., 2023; Tavana Amlashi et al., 2023). These models have outperformed traditional regression methods in estimating concrete properties, including slump and strength parameters (Albaijan et al., 2023). For instance, Tavana Amlashi et al. (Tavana Amlashi et al., 2023) demonstrated that ANN achieved superior accuracy in predicting the workability and strength of BPC. Ghanizadeh et al. (2019) also confirmed the effectiveness of artificial neural networks prediction sort vector machines (SVM) in modeling BPC behavior, with cement content emerging as the most dominant input parameter influencing the predictions. A hybrid modeling strategy that ANN, support vector machines, and adaptive neuro-fuzzy inference systems with particle swarm optimization demonstrated notable improvements in predictive accuracy, with the ANN-PSO configuration attaining a coefficient of determination

(R^2) of 0.95 (Tavana Amlashi et al., 2020). Other techniques, including response surface methodology (RSM), multiple gene genetic programming (MGGP), and group method of data handling (GMDH), have also shown effectiveness in estimating compressive strength (Amlashi et al., 2022).

The second stream involves ensemble learning (EL) methods including Random Forest (RF), Gradient Boosting Regression Trees (GBRT), and Extreme Gradient Boosting (XGB). In a study tested six algorithms including XGB, RF, and KNN to predict BPC compressive strength using components like water, sand, cement, and bentonite. Their findings showed EL methods consistently outperformed standalone models across various metrics (Zhou, 2012). Ensemble learning (EL) techniques have also shown strong predictive capabilities across various concrete formulations, including high-performance concrete (Ekanayake et al., 2022; Rathakrishnan et al., 2022), recycled aggregate concrete (Ekanayake et al., 2022; Zeng et al., 2022), lightweight foamed concrete (H. S. Ullah et al., 2022), geopolymer concrete (Eftekhar Afzali et al., 2024), self-compacting concrete (Hoang, 2022), and rice husk ash concrete (Alyami et al., 2024). Stacked ensemble models employing Extreme Gradient Boosting (XGB) as the base learner and linear regression as the meta-learner have been shown to enhance prediction accuracy by effectively combining the strengths of both algorithms. Boosting techniques like adaptive boosting (ADB) and bagging algorithms like RF enhance generalization through weighted sampling and residual error minimization (Iftikhar et al., 2022).

The third research stream integrates optimization techniques for hyperparameter tuning to improve model accuracy and robustness. Approaches such as PSO and forensic-based investigation optimization (FBIO) automate parameter selection and reduce computational complexity (Y. Yang et al., 2024). While hyperparameter tuning is often computationally demanding, recent studies have demonstrated that integrating FBIO with boosting and bagging methods significantly enhances efficiency and prediction quality (H. Yang et al., 2022).

This study aims to develop an accurate and interpretable machine learning framework for predicting key mechanical properties of bentonite plastic concrete (BPC), including slump, tensile strength, and elastic modulus. By integrating four ensemble learning models with Forensic-Based Investigation Optimization (FBIO), the research enhances predictive performance and ensures robustness across diverse datasets.

While previous studies have demonstrated the effectiveness of standalone, ensemble, and optimization-enhanced ML models in predicting the mechanical properties of various concrete types, several key limitations remain unresolved. Most existing models prioritize predictive accuracy over interpretability, making it difficult to extract meaningful insights for material design and process optimization. Moreover, issues such as data imbalance, small dataset size, overfitting, and computational burden hinder their applicability to real-world BPC systems, which exhibit strong nonlinearity and compositional variability. Few studies have focused specifically on bentonite plastic concrete, particularly in the context of sustainability and environmental engineering. To bridge these gaps, the present study proposes an interpretable and optimized ensemble learning framework integrated with forensic-based investigation optimization (FBIO) to achieve high predictive accuracy with enhanced transparency and robustness. This approach not only advances the digital transformation of construction materials research but also supports sustainable engineering practices by reducing experimental workloads, optimizing material use, and contributing to environmentally responsible infrastructure development.

3. Research Methodology

To develop robust and generalizable predictive models for slump, tensile strength, and elastic modulus of bentonite plastic concrete (BPC), this study adopts an optimized ensemble learning framework enhanced by forensic-based investigation optimization (FBIO). The methodological flow is illustrated in Fig. 1, outlining each critical stage from data preprocessing to final model deployment. Initially, raw experimental datasets were normalized and randomly partitioned into training (70%) and testing (30%) subsets. The training dataset was then utilized to encode hyperparameters for four ensemble learning (EL) models Adaptive Boosting (ADB), Gradient Boosting Regression Trees (GBRT), Extreme Gradient Boosting (XGB), and Random Forest (RF) covering key configurations such as learning rate, estimators, and splitting criteria.

FBIO was employed to optimize these hyperparameters through a simulation of investigative strategies that navigate the search space without manual intervention. After training, the EL models were evaluated using a multi-objective performance function and validated against the unseen testing data. The final hybridized models were saved and prepared for application deployment to assist engineers in real-time BPC performance forecasting. This comprehensive approach ensures not only high predictive accuracy but also interpretability and practical relevance.

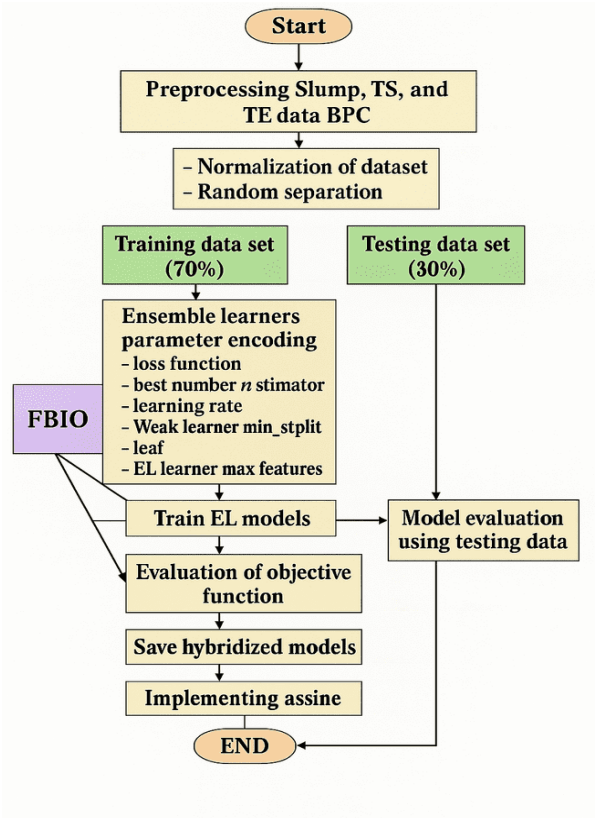

Fig. 1. Methodological framework for predicting BPC performance using optimized ensemble learning models integrated with FBIO.

3.1 Data Acquisition and Preprocessing

This study utilized three separate databases comprising 130, 170, and 120 observations related to TS, E, and S of BPC, respectively (Abbaslou et al., 2016; Al-Luhybi & Qader, 2021; Alós Shepherd & Dehn, 2023; Amlashi et al., 2019; Faraj et al., 2020; Guan & Zhang, 2011; Hameed et al., 2023; L. Hu et al., 2012; L. M. Hu et al., 2014; Mahboubi & Ajorloo, 2005; Mousavi et al., 2012; Nafees et al., 2023; Pisheh & Mir Mohammad Hosseini, 2012; Svetnik et al., 2003; Wu et al., 2020; P. Zhang et al., 2013). These datasets were compiled from established experimental studies and curated to ensure consistency in measurement units and formats. To harmonize compressive strength values derived from different specimen geometries, UNESCO conversion coefficients proposed by Elwell & Fu (1995) were employed to normalize cylindrical and cube test results.

The key input parameters selected for this investigation include the quantities of gravel, sand, cement, bentonite, silty clay, and water, along with the curing duration. As depicted in Fig. 2, the datasets exhibit a non-uniform and skewed distribution across all target variables highlighting the presence of class imbalance and variability. For slump (S-BPC), most data points are concentrated in the 20–24 cm range, representing over 50% of the samples, while lower slump values (4–16 cm) are sparsely represented. Similarly, tensile strength (TS-BPC) values are heavily skewed toward lower strengths, with over 60% of the samples clustered around 0.4 MPa, and a steep decline in frequency for higher strength levels. In the case of elastic modulus (E-BPC), the

dataset is dominated by values in the 1–2 GPa range, with only a few instances reaching 6–8 GPa. This distributional imbalance emphasizes the complexity and heterogeneity of the BPC dataset, reinforcing the necessity for robust models capable of generalizing across underrepresented and high-variance instances, thereby enhancing their applicability to diverse, real-world construction scenarios (Iqbal et al., 2020).

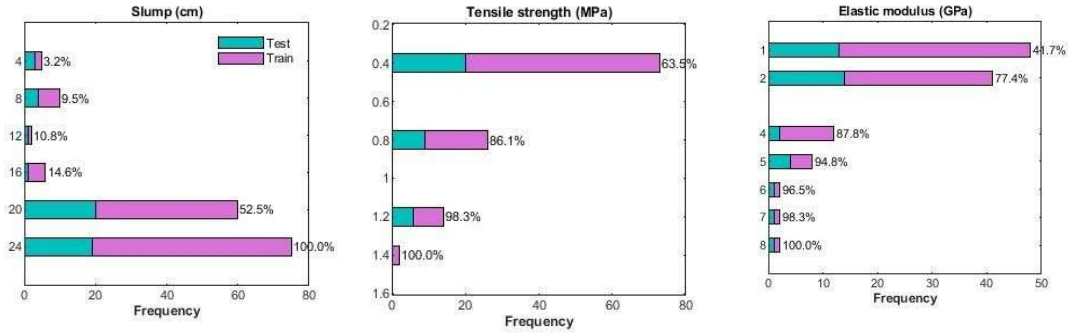

Fig. 2. Frequency distribution histograms of output variables for training and testing datasets.

Correlation analysis, as depicted in Fig. 3, reveals varying degrees of linear relationships between the input parameters and the key performance indicators of BPC, namely slump, TS, and E. The correlation heatmap for slump shows that this fresh property is weakly influenced by the primary aggregates. Specifically, slump is negatively correlated with gravel (−0.15) and positively associated with silt (0.25) and bentonite (0.40), suggesting that finer particles and bentonite enhance workability. The correlation with water content is relatively low (0.17), indicating a more complex interaction in the presence of bentonite and other fines.

In contrast, tensile strength exhibits a strong positive correlation with curing time (0.87), followed by water content (0.74), highlighting the critical role of extended hydration and moisture in strength development. Additionally, moderate positive correlations with gravel (0.48), cement (0.43), and bentonite (0.40) reflect the contribution of both aggregate structure and binder content in enhancing tensile behavior. These findings underscore the multifactorial nature of strength formation in BPC systems.

Elastic modulus also correlates most significantly with curing time (0.54), followed by cement (0.46) and silt (0.44), suggesting that long-term hydration and the presence of fine particles enhance the stiffness of the composite. Correlations with water (0.07) and gravel (−0.29) are weak or negative, implying limited or adverse influence on elastic properties. Collectively, these correlation insights demonstrate that slump is primarily governed by fine materials and bentonite content, tensile strength is predominantly influenced by curing time and moisture availability, while elastic modulus depends more on cementitious content and the duration of curing. This analysis forms the basis for informed feature selection in predictive modeling and mix design optimization for BPC.

Prior to model training, each dataset was randomly partitioned into training (70%) and testing (30%) subsets to facilitate model development and validation. Descriptive statistical analysis was conducted on the training data to evaluate the distribution characteristics of input and output variables. Fig. 4 present the statistical summaries for the S–BPC, TS–BPC, and E–BPC datasets, respectively. These summaries include essential metrics such as minimum, maximum, mean, median, standard deviation, variance (for E–BPC), skewness, and kurtosis. The inclusion of these statistical descriptors ensures that each dataset captures a realistic range of values while providing insights into central tendency, dispersion, and distribution shape. This step is critical for identifying outliers, assessing data balance, and ensuring appropriate conditions for machine learning model training and evaluation (Iqbal et al., 2020).

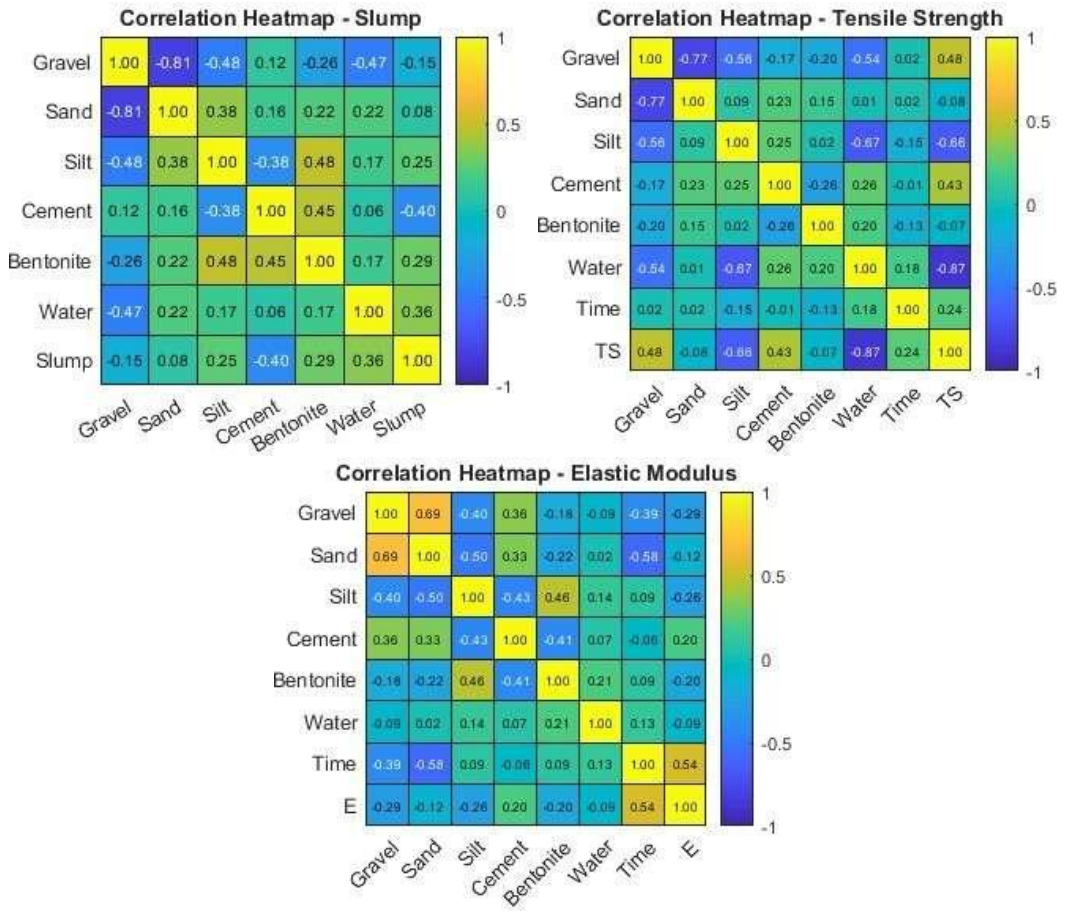

Fig. 3. Correlation heatmaps illustrate the relationship between input parameters and target properties.

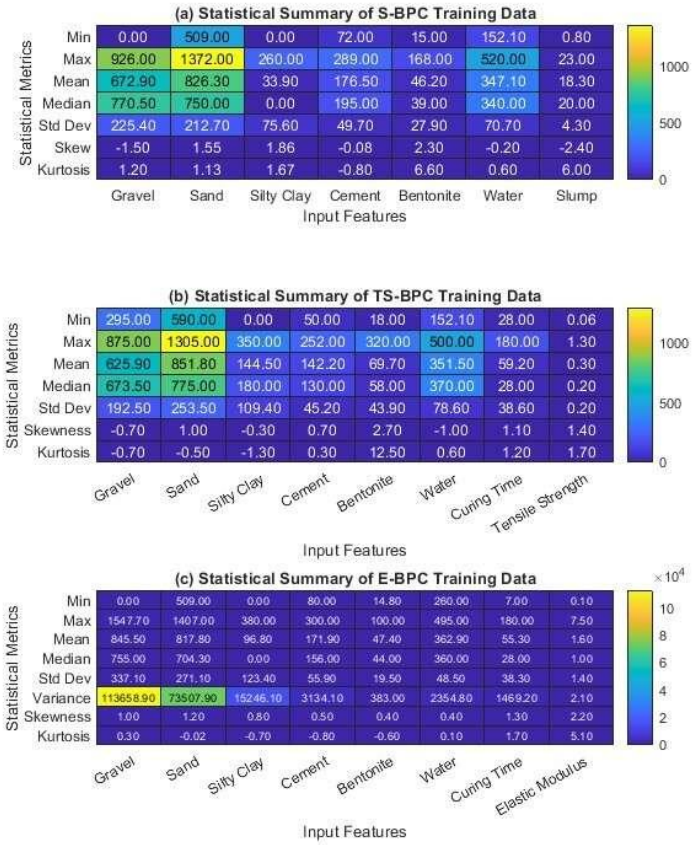

Fig. 4. present the statistical summaries for the datasets.

The effective input parameter ranges used for model development were determined by selecting the highest minimum and the lowest maximum values observed across all datasets. This approach ensured consistency and logical applicability of the models within valid operational limits. Finally, the diversity in data sources and output variation underlines the generalization capability of the developed models across multiple experimental conditions and construction contexts (Tavana Amlashi et al., 2023).

3.2 Adaptive Models

This section outlines the ensemble learning algorithms employed to predict the mechanical properties of bentonite plastic concrete (BPC). Four advanced models Adaptive Boosting (ADB), Gradient Boosting Regression Trees (GBRT), Extreme Gradient Boosting (XGB), and Random Forest (RF) were selected for their proven ability to handle complex, nonlinear relationships and improve generalization through ensemble strategies. Each algorithm was integrated with Forensic-Based Investigation Optimization (FBIO) to fine-tune hyperparameters, enhance predictive accuracy, and reduce overfitting. The following subsections describe the structure and working principles of each model within the optimized learning framework.

3.2.1 Adaptive Boosting-Based Learning (ADB)

Adaptive Boosting, originally conceptualized by Schapire (1990), enhances the performance of weak classifiers by sequentially re-weighting training samples. In each iteration, misclassified instances are assigned higher weights to guide subsequent learners toward these harder-to-classify points (CAO et al., 2013; Schapire, 2009). Typically using decision trees due to their simplicity and interpretability (Safavian & Landgrebe, 1991), ADB aggregates multiple weak learners into a single, robust model. The additive model describes by formula (1).

$$Fn(x) = Fn - 1(x) + argmin_h \sum_{i=1}^{n} L\left(yi, F_{n-1}(x_i) + h(x_i)\right) \quad (1)$$

Where $F_n(x_i)$denotes the nth iteration model, $h(x_i)$represents the new weak learner, and L is the loss function.

The working mechanism of ADB is visually summarized in Fig. 5., where each iteration updates the weight distribution based on misclassifications, leading to improved performance in the composite model. Each weak learner G_i is trained with a specific sample weighting w_i, updated iteratively to penalize misclassification. After all weak learners are trained, they are combined using a weighted majority vote to form the final strong classifier H. This mechanism ensures that the model progressively improves by learning from its mistakes at each stage.

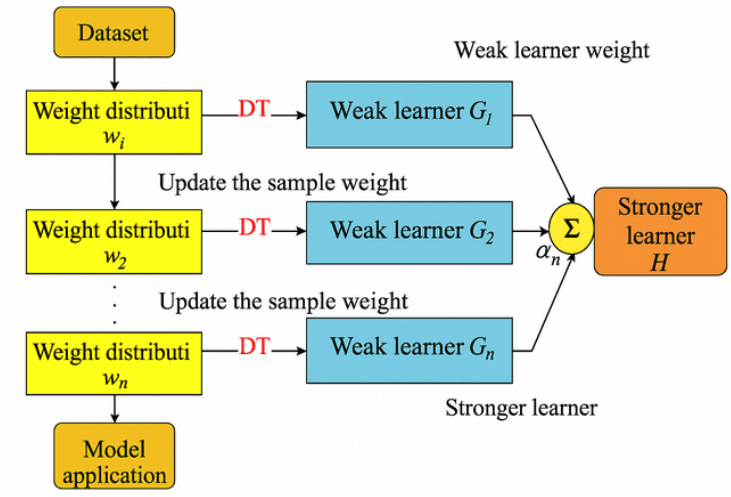

Fig. 5. Schematic representation of the Adaptive Boosting (ADB) process.

3.2.2 Gradient Boosting Regression Trees (GBRT)

GBRT integrates gradient descent optimization with regression trees, initially proposed through the CART framework by Breiman et al. (2017). In this model, each tree is trained to minimize residuals of the prior learners. Its structure recursively divides the feature space and assigns prediction values $c_{m,j}$ to each region $R_{m,j}$ as in formula (2).

$$F_m(x) = F_{m-1}(x) + \sum_{j=1}^{J_m} c_{m,j}\, I(x \in R_{m,j}) \quad (2)$$

Here, $I(x \in R_{m,j})$ is an indicator function denoting membership within a region.

Fig. 6. illustrates the GBRT architecture. The model begins by fitting a weak learner to the initial dataset, computing residuals (gradients) and updating the ensemble iteratively. Each new tree attempts to capture the remaining patterns in the error terms, and the outputs are combined into a strong predictive model through additive updates.

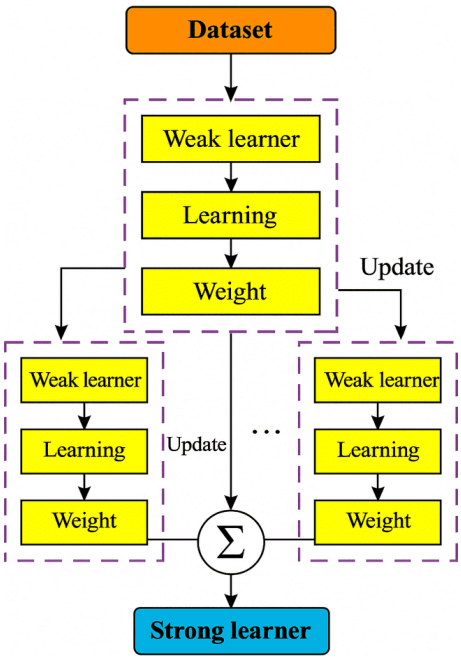

Fig. 6. Structural flow of the Gradient Boosting Regression Trees (GBRT) algorithm.

3.2.3 Extreme Gradient Boosting (XGB)

XGB is an optimized version of gradient boosting, designed for computational speed and scalability (Chen & He, 2014). It minimizes a regularized objective function comprising a convex loss function and a complexity penalty and it expressed by formula (3).

$$L_{(t)} = \sum_{i=1}^{n} l(y_i, y_i^{(t-1)} + f_t(x_i)) + \Omega(f_t) \quad (3)$$

Where l denotes the loss function between predicted y_i and actual values y_i, while $\Omega(f_t)$, the regularization component, is given by formula (4).

$$\Omega(f_k) = \gamma T + \frac{1}{2}\lambda \parallel w \parallel^2 \quad (4)$$

This formulation encourages model simplicity and avoids overfitting. Fig. 7. illustrates the iterative structure of XGB, where successive trees are constructed to fit the residual errors from the previous iteration. Each tree contributes incrementally to the ensemble, thereby refining predictions and reducing loss in a controlled manner.

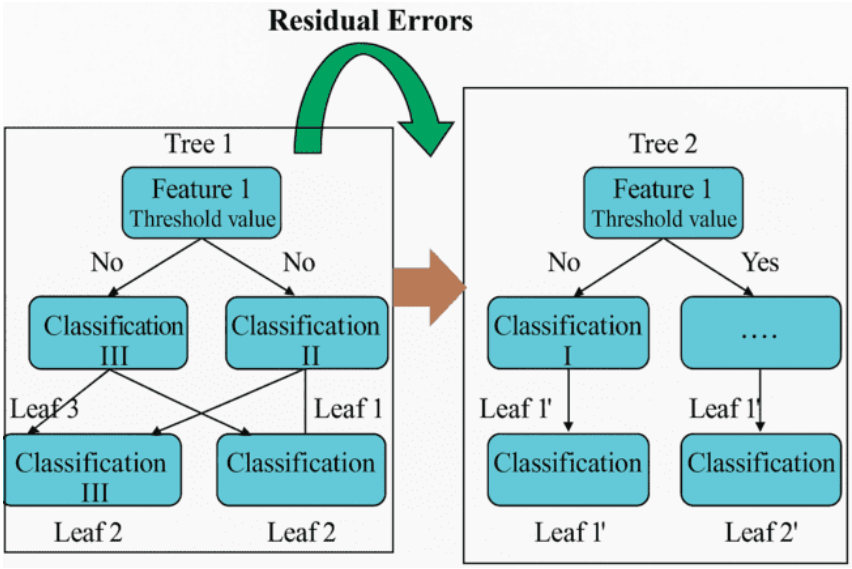

Fig. 7. Conceptual diagram of Extreme Gradient Boosting (XGB).

3.2.4 Random Forest (RF)

Random Forest (RF), as proposed by Svetnik et al. (2003), is an ensemble-based regression algorithm that generates multiple decision trees through bootstrapped samples and random feature selection. Each tree is independently trained, and the final prediction is derived from the average of all tree outputs. This technique reduces variance and enhances the model's generalization capacity. Fig. 8. illustrates the structure of the Random Forest algorithm. It begins with the training dataset and generates several sub-models through bootstrap sampling. Each sub-model (decision tree) learns independently and provides an individual prediction. These predictions are then aggregated via voting or averaging to yield the final model output. The predictive function of RF can be represented as in formula (5).

$$M(x) = \frac{1}{N}\sum_{i=1}^{n} y_i\,(x, \theta_n) \tag{5}$$

Where θ_n indicates the parameters and training subsets used for individual trees (J. Zhang et al., 2024).

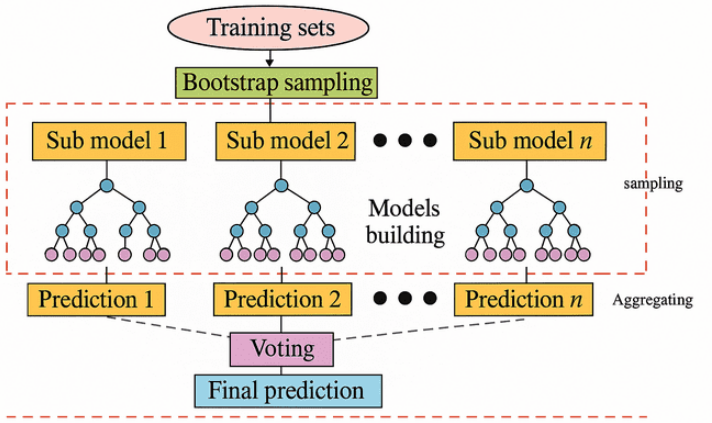

Fig. 8. Random Forest learning architecture.

3.2.5 Forensic-Based Investigation Optimization (FBIO)

Metaheuristic optimization techniques are widely applied in machine learning for hyperparameter tuning, with notable methods including Genetic Algorithms (GA), Particle Swarm Optimization (PSO), and Whale Optimization Algorithm (WOA) (Ly et al., 2021). The Forensic-Based Investigation Optimization (FBIO) method, introduced by Chou & Nguyen (2020), stands apart by simulating the procedures of criminal investigations. In FBIO, the optimization domain is conceptualized as a search area, the optimal solution is termed the

"culprit", and search agents are metaphorically represented as investigators. Importantly, FBIO does not require manual configuration of internal control parameters, simplifying the optimization process (Moghaddam et al., 2025).

FBIO proceeds in two primary stages: an initial search (Stage P), where potential solutions are evaluated, and a convergence phase, wherein the best candidate solution analogous to identifying the culprit is iteratively refined. This approach enables automatic tuning of ensemble learning models, improving prediction accuracy while reducing the computational burden traditionally associated with manual hyperparameter selection (Qu et al., 2021). As illustrated in Fig. 9., the algorithm is divided into two operational teams. The Investigation Team (blue) initially updates and expands the most promising regions of the search space. The Pursuit Team (red) then bounds and intensifies the search around the most suspected zones. The iteration continues until a predefined stopping criterion is met, typically the maximum number of iterations, after which the “culprit” (the optimal solution) is identified and selected.

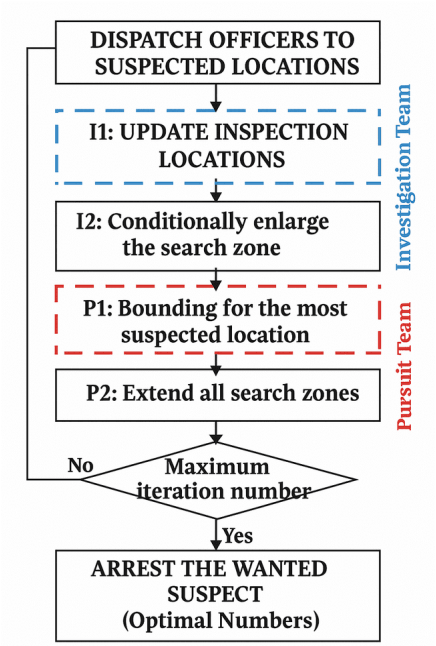

Fig. 9. Forensic-Based Investigation Optimization (FBIO) algorithm flow

3.3 Meta-Parameter Optimization and Model Configuration

The meta-parameter optimization for each ensemble learning algorithm was conducted using the FBIO strategy, targeting three predictive tasks: S-BPC, TS-BPC, and E-BPC of bentonite plastic concrete. The meta-parameters were rigorously tuned within predefined ranges to ensure model generalizability and performance.

The hyperparameter search space was extensively designed to accommodate a diverse range of values, customized for each ensemble model. Core parameters included the number of estimators (ranging from 5 to 200), maximum tree depth (2 to 500), and maximum number of leaf nodes (2 to 500). For the Random Forest (RF) models, min_samples_split and min_samples_leaf were defined in a discrete range from 1 to 10. In contrast, for other models, these parameters were defined in a continuous search space between 1e-10 and 1. Additional critical hyperparameters optimized in the boosting-based models.

Each ensemble model was uniquely configured to match the slump prediction data characteristics as in Table 1. ADB-FBIO used 29 estimators with a deep max depth of 268 and lightweight splitting thresholds (min_samples_split and min_samples_leaf ≈ 0.003), relying on a single input feature. GBRT-FBIO utilized 75 estimators, a max depth of 120, learning rate of 0.35, three features, and a subsample ratio of 0.5. XGB-FBIO employed 64 estimators, an extremely deep tree (max_depth = 500), and a high learning rate of 0.78. RF-FBIO achieved optimal results

with only 10 estimators, a deep max depth of 446, min_samples_split = 2, and max_samples = 0.89.

Table 1 - S-BPC Ensemble Model Configurations

Model	Estimators	Max Depth	Learning Rate	Features	Subsample	Min Split	Max Samples
ADB-FBIO	29	268	–	1	–	≈ 0.003	–
GBRT-FBIO	75	120	0.35	3	0.5	–	–
XGB-FBIO	64	500	0.78	–	–	–	–
RF-FBIO	10	446	–	–	–	2	0.89

For TS-BPC models as in Table 2., ADB-FBIO utilized 28 estimators with a moderately deep structure (max_depth = 64) and a learning rate of 0.25. GBRT-FBIO incorporated 47 estimators, a deeper tree (max_depth = 131), learning rate of 0.36, and a relatively high subsample of 0.79. XGB-FBIO had an extensive configuration with 185 estimators, max_depth = 472, and a learning rate of 0.61. RF-FBIO applied 128 estimators, max_depth = 481, min_samples_split = 4, and max_samples = 0.95.

Table 2 - TS-BPC Ensemble Model Configurations

Model	Estimators	Max Depth	Learning Rate	Subsample	Min Split	Max Samples
ADB-FBIO	28	64	0.25	–	–	–
GBRT-FBIO	47	131	0.36	0.79	–	–
XGB-FBIO	185	472	0.61	–	–	–
RF-FBIO	128	481	–	–	4	0.95

For E-BPC models, the ADB-FBIO model adopted a compact setup with only 7 estimators as in Table 3, a significant depth (max_depth = 227), and a learning rate of 0.42. GBRT-FBIO employed 44 estimators, max_depth = 298, learning rate of 0.59, alpha = 0.05, and a high subsample ratio of 0.98. XGB-FBIO achieved high learning efficiency with 16 estimators, max_depth = 254, and a learning rate of 1.36. RF-FBIO applied just 5 estimators but used an extremely deep model (max_depth = 499), max_features = 7, max_samples = 0.97, and a pruning parameter ccp_alpha = 1.42.

Table 3- E-BPC Ensemble Model Configurations

Model	Estimators	Max Depth	Learning Rate	Subsample	Max Features	Max Samples	Alpha	ccp_alpha
ADB-FBIO	7	227	0.42	–	–	–	–	–
GBRT-FBIO	44	298	0.59	0.98	–	–	0.05	–
XGB-FBIO	16	254	1.36	–	–	–	–	–
RF-FBIO	5	499	–	–	7	0.97	–	1.42

These optimized configurations clearly demonstrate the versatility and adaptability of ensemble learners when tuned using the FBIO algorithm. Each model was effectively tailored to reflect the underlying structure of the target variables Slump, Tensile Strength, and Total Elongation yielding high predictive accuracy while maintaining interpretability. The diverse

parameter settings underline the complexity and heterogeneity in concrete behavior, emphasizing the importance of domain-specific tuning in predictive modeling.

To ensure data consistency, all input variables were normalized using Z-score normalization, which standardizes features by centering their mean at zero and scaling their standard deviation to one, thereby enhancing numerical stability and convergence during model training. The dataset was randomly partitioned into 70% training and 30% testing subsets to maintain statistical representativeness and prevent sampling bias. Feature selection was guided by correlation analysis and domain relevance, ensuring that only parameters with meaningful physical and statistical relationships to BPC performance were retained, while redundant or weakly correlated variables were excluded to improve model efficiency. The choice of the four ensemble algorithms ADB, GBRT, XGB, and RF was based on their proven capability to model nonlinear and heterogeneous materials, offering complementary strengths in variance reduction, bias correction, and generalization. The Forensic-Based Investigation Optimization (FBIO) algorithm was specifically selected due to its self-adaptive search mechanism, which eliminates manual parameter tuning and efficiently identifies optimal hyperparameters with lower computational cost compared to conventional metaheuristics such as PSO or GA. This integration of robust ensemble learning with an adaptive optimizer provides a balanced framework that enhances accuracy, interpretability, and computational efficiency for predicting the mechanical properties of BPC.

3.4 Model Efficiency Assessment Specifications

To evaluate the performance and predictive accuracy of the developed machine learning models, several well-established statistical error metrics were employed. These include the coefficient of determination (R^2), mean absolute error (MAE), root mean square error (RMSE), mean absolute percentage error (MAPE), the a20-index, and a composite objective function (OBJ). The equations and their respective formulations are presented below:

3.4.1. Coefficient of Determination (R^2)

The R^2 metric assesses how well the predicted values approximate the actual observed outcomes (Turney, 2022). It is defined as in formula (6).

$$R^2 = \left[\frac{\sum_{i=1}^{N} (\mathrm{Y_{obs}} - \bar{\mathrm{Y}}_{\mathrm{obs}})(\mathrm{Y_{pre}} - \bar{\mathrm{Y}}_{\mathrm{pre}})}{\sqrt{\sum_{i=1}^{N} (\mathrm{Y_{obs}} - \bar{\mathrm{Y}}_{\mathrm{obs}})^2 \sum_{i=1}^{N} (\mathrm{Y_{pre}} - \bar{\mathrm{Y}}_{\mathrm{pre}})^2}} \right] \quad (6)$$

Where $\mathrm{Y_{obs}}$ is the observed value. $\mathrm{Y_{pre}}$ is the predicted value. $\bar{\mathrm{Y}}_{\mathrm{pre}}$ and $\bar{\mathrm{Y}}_{\mathrm{obs}}$ are the mean values of observed and predicted data, respectively. N is the number of data points

3.4.2. Mean Absolute Error (MAE)

MAE quantifies the average absolute difference between predicted and observed values (Karunasingha, 2022) as in formula (7).

$$MAE = \frac{\sum_{i=1}^{N} |\mathrm{Y}_{pre} - \mathrm{Y_{obs}}|}{N} \quad (7)$$

3.4.3. Mean Absolute Percentage Error (MAPE)

MAPE provides a normalized measure of prediction error in percentage terms (de Myttenaere et al., 2016) as in formula (8).

$$MAPE = \frac{\sum_{i=1}^{N} |\mathrm{Y}_{pre} - \mathrm{Y_{obs}}|}{\sum_{i=1}^{N} \mathrm{Y_{obs}}} \times 100\% \quad (8)$$

3.4.4. Root Mean Square Error (RMSE)

RMSE evaluates the square root of the average of squared differences between predicted and observed values (Karunasingha, 2022) as in formula (9).

$$RMSE = \sqrt{\frac{1}{N}\sum_{i=1}^{N}\left(\mathrm{Y}_{pre} - \mathrm{Y}_{\mathrm{obs}}\right)^2} \quad (9)$$

3.4.5. Objective Function (OBJ)

The composite objective function integrates both training and testing error metrics and model accuracy (Sahoo et al., 2019). It is expressed as in formula (10).

$$OBJ = \left(\frac{N_{tr}}{N_{all}} \times \frac{RMSE_{tr}+MAE_{tr}}{R_{tr}^2+1}\right) + \left(\frac{N_{tst}}{N_{all}} \times \frac{RMSE_{tst}+MAE_{tst}}{R_{tr}^2+1}\right) \quad (10)$$

Where, N_{tr} and N_{tst}denote the number of training and testing data points, respectively. Also N_{all}=N_{tr}+N_{tst}.

3.4.5. a20-Index

The a20-index measures the proportion of predictions that fall within ±20% of the actual values (Xu et al., 2019), defined as in formula (11).

$$a20 - index = \frac{m20}{N} \quad (11)$$

Where m20 is the number of predicted values within ±20% of the observed values. N is the total number of predictions

4. Result and Dissuasion

This section presents the outcomes of the predictive modeling and performance evaluation processes conducted on bentonite plastic concrete (BPC) using FBIO-optimized ensemble learning algorithms. Following the training and validation of the models, the results are systematically analysed to assess their predictive accuracy, robustness, and generalization capability. Various statistical indicators and validation techniques are employed to ensure comprehensive evaluation across different mechanical properties. In addition to quantitative performance metrics, model interpretability is addressed using feature attribution methods. The discussions aim to contextualize these results within the broader scope of intelligent concrete performance modeling and highlight the practical implications for engineering applications.

4.1 Model Prediction Accuracy Study

The predictive performance of the proposed hybrid ensemble models was rigorously assessed using several statistical indicators, including R^2, RMSE, MAE, MAPE, a20-index, OBJ, Scatter Index (SI), and Nash–Sutcliffe Efficiency (NSE). These metrics were applied to both training and testing datasets to ensure reliable evaluation of model generalizability and accuracy.

Fig. 10 illustrates the predictive performance of four FBIO-optimized ensemble models in estimating the slump values of bentonite plastic concrete (BPC). All models achieved high coefficient of determination (R^2) values in both training and testing phases, indicating strong predictive capability. Among them, the AdaBoost–FBIO model achieved the highest training accuracy (R^2 = 0.999) and testing performance (R^2 = 0.972), along with the lowest RMSE and MAE values, and perfect a20 accuracy (1.000 in training, 0.910 in testing). Similarly, XGBoost–FBIO and GBRT–FBIO models demonstrated excellent generalization, with testing R^2 values of 0.976, and testing a20 accuracies of 0.946 and 0.947, respectively. While RF–FBIO also performed reasonably well, it exhibited slightly higher error metrics (RMSE = 1.607; MAE = 1.139 in testing) and the lowest testing a20 accuracy (0.877), suggesting comparatively reduced precision. These findings confirm the robustness of the FBIO-optimized boosting models, especially AdaBoost and XGBoost, in accurately predicting the fresh property behavior of BPC.

Fig. 11 presents the performance of four FBIO-tuned ensemble models in predicting the tensile strength of bentonite plastic concrete (TS-BPC). All models demonstrate strong predictive ability, with high R^2 values and low RMSE and MAE scores in both training and testing phases. Notably, the XGBoost–FBIO model achieved the highest accuracy, with an R^2 of 0.999 (training) and 0.987 (testing), accompanied by extremely low RMSE (0.003 in training, 0.031 in testing) and MAE (0.001 and 0.034, respectively), as well as perfect a20 accuracy during training. This confirms its exceptional capability in learning nonlinear patterns.

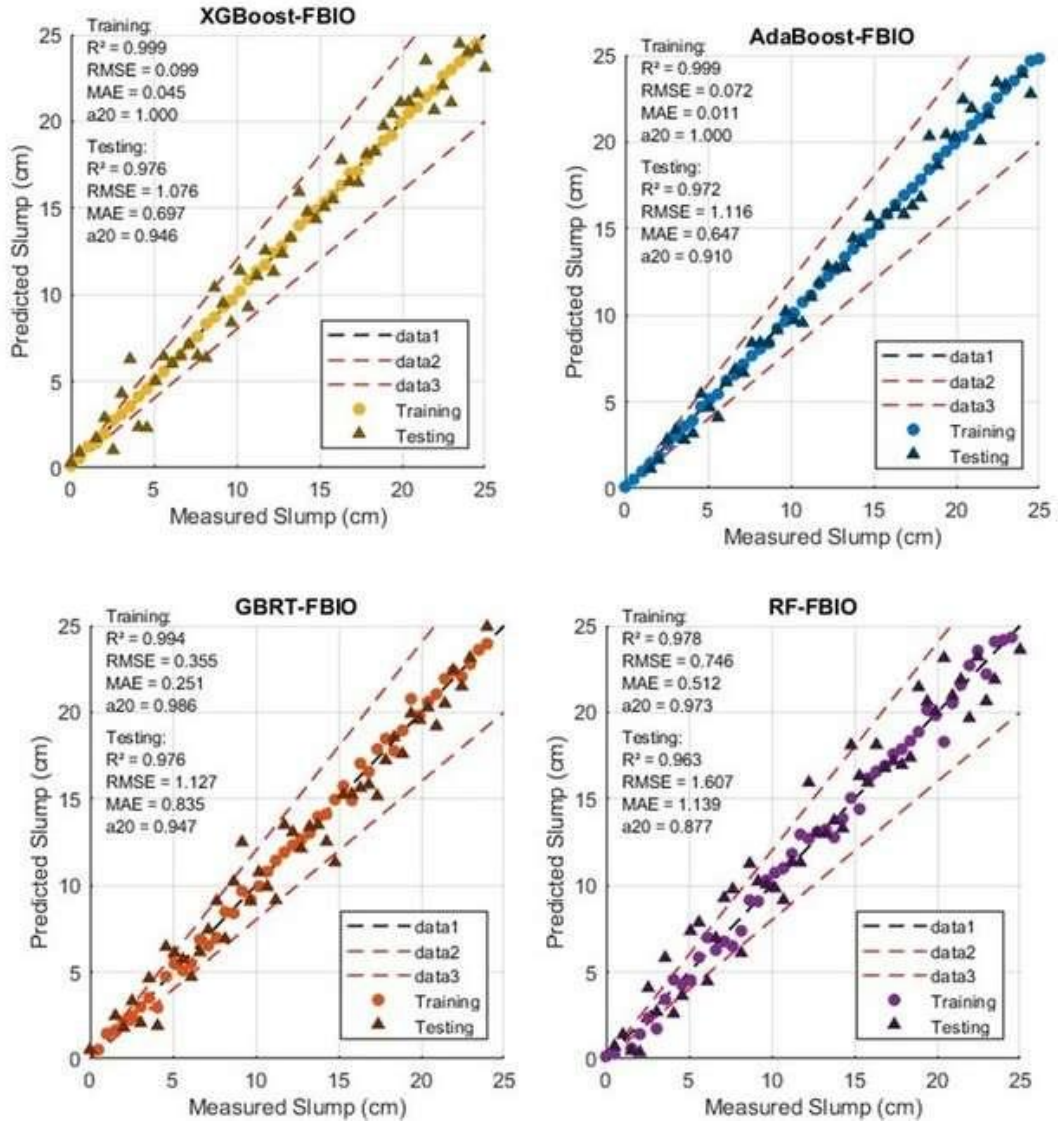

Fig. 10. Predicted versus measured slump values for FBIO-optimized ensemble models: AdaBoost, GBRT, XGBoost, and Random Forest (RF)

The GBRT–FBIO model closely followed, with a training R^2 of 0.997 and testing R^2 of 0.978, and similarly favorable error metrics. AdaBoost–FBIO also performed reliably, though with slightly reduced a20 accuracy in the testing phase (0.721). In comparison, the RF–FBIO model yielded lower predictive accuracy, with higher RMSE and MAE values, particularly during training (RMSE = 0.055, MAE = 0.042). Overall, XGBoost–FBIO and GBRT–FBIO exhibited the most reliable and generalizable performance for tensile strength prediction, underscoring their suitability for mechanical property modeling in BPC systems.

Fig. 12 compares the predictive performance of FBIO-optimized AdaBoost, GBRT, XGBoost, and Random Forest models in estimating the elastic modulus of bentonite plastic concrete (E-BPC). The GBRT–FBIO model emerged as the most effective predictor, achieving a

training R^2 of 0.999 and a testing R^2 of 0.974, with low RMSE (0.032 training, 0.279 testing) and MAE values, and a strong a20-index of 0.975 in training.

The XGBoost–FBIO model also demonstrated excellent learning capacity during training (R^2 = 0.999, a20 = 1.000), but its generalization performance declined moderately in testing, with an a20-index of 0.555 and a higher RMSE of 0.442. The AdaBoost–FBIO model showed solid results (R^2 = 0.989 training, 0.914 testing), although its a20-index in testing dropped to 0.711. Among all models, the RF–FBIO exhibited the weakest predictive accuracy, particularly in testing, with an R^2 of 0.880, RMSE of 0.625, and the lowest a20-index of 0.444. These results underscore the superior consistency and accuracy of the GBRT–FBIO model for modeling the elastic modulus of BPC, with XGBoost being competitive in training but less robust in generalization.

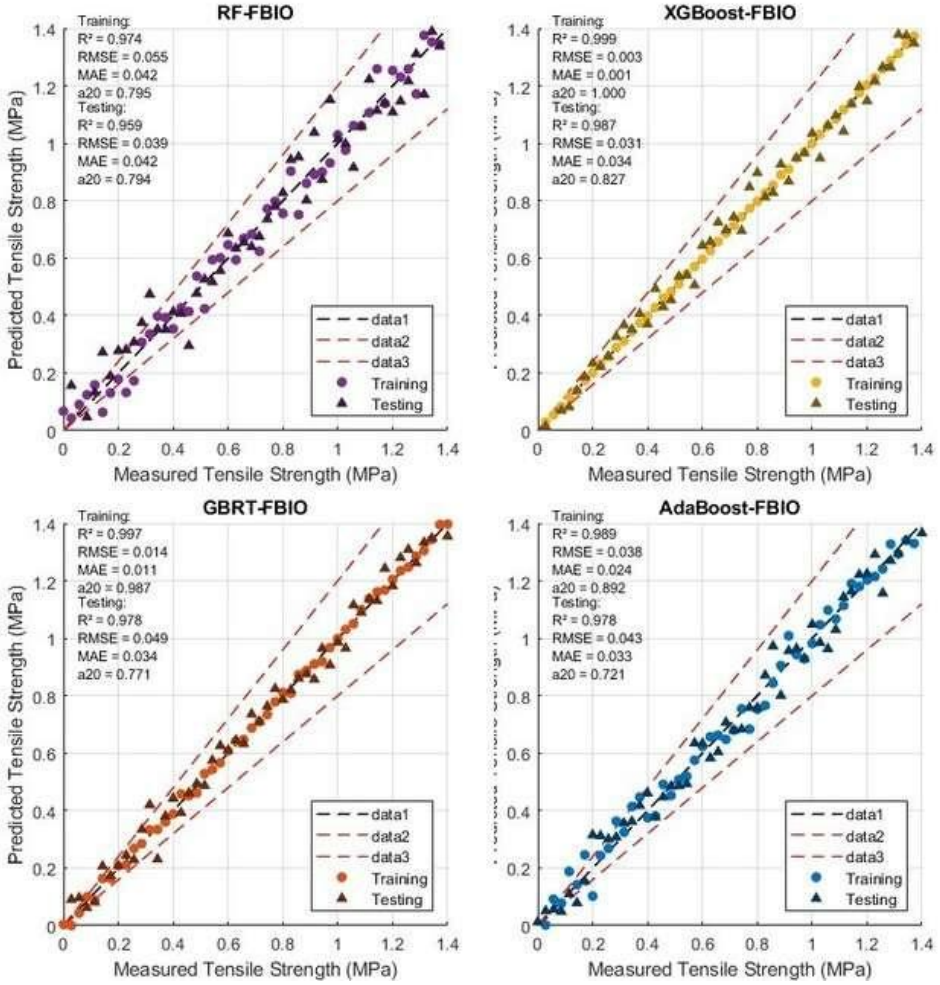

Fig. 11. Predicted versus measured tensile strength (TS) values for FBIO-optimized ensemble models: AdaBoost, GBRT, XGBoost, and Random Forest (RF).

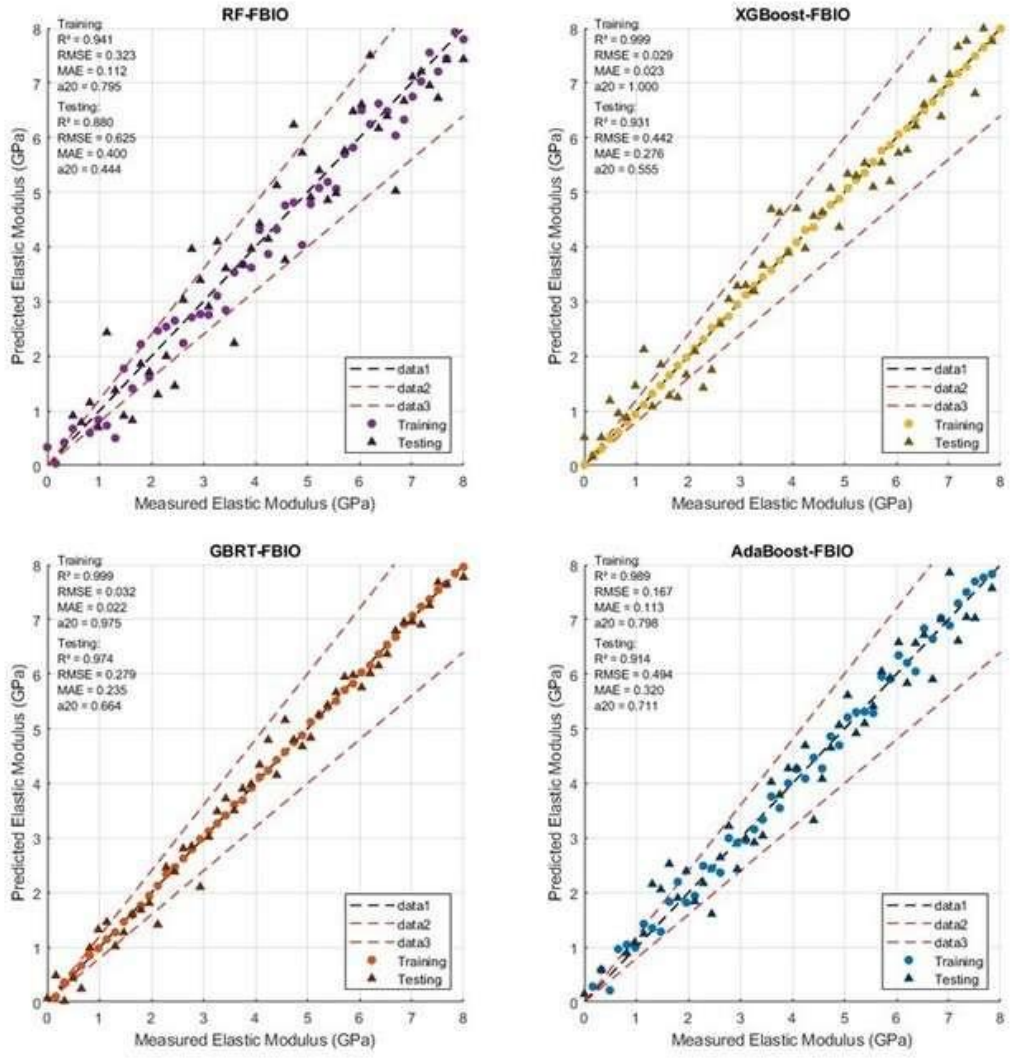

Fig. 12. Predicted versus measured elastic modulus (E) values for FBIO-optimized ensemble models: AdaBoost, GBRT, XGBoost, and Random Forest (RF).

To benchmark comparative performance, Fig. 13 presents a consolidated evaluation of key error metrics and goodness-of-fit indicators across all FBIO-optimized models. In the S-BPC training phase, AdaBoost–FBIO demonstrated the lowest RMSE (0.072 cm), outperforming GBRT, XGBoost, and RF by margins of 0.283 cm, 0.027 cm, and 0.674 cm, respectively. However, in the testing phase, XGBoost–FBIO achieved the best performance with the lowest RMSE (1.076 cm), slightly outperforming AdaBoost, GBRT, and RF by 0.04 cm, 0.051 cm, and 0.531 cm, respectively.

While numerical accuracy provides a quantitative measure of model performance, its engineering interpretation reveals deeper insights into BPC behavior. The results indicate that the ensemble models effectively capture the nonlinear interactions among cement, bentonite, and water content, which directly influence hydration, microstructural densification, and pore connectivity. Higher cement proportions enhanced the load-bearing matrix and strength development, whereas increased bentonite content improved workability and impermeability up to a critical threshold beyond which excessive swelling led to reduced stiffness. These findings confirm that the proposed ML framework reflects the actual material mechanisms governing BPC's mechanical performance rather than serving purely as a predictive tool.

To statistically verify the performance differences among the models, an analysis of variance (ANOVA) test was conducted on the cross-validation results. The F-statistic indicated that the mean prediction errors differed significantly across models ($p < 0.05$), confirming that the superior performance of XGB and GBRT was not due to random variation. Post-hoc Tukey

analysis further validated that these two algorithms significantly outperformed RF and ADB models in terms of RMSE and MAE. This confirms that the improvements achieved through ensemble boosting are statistically meaningful and robust across the dataset.

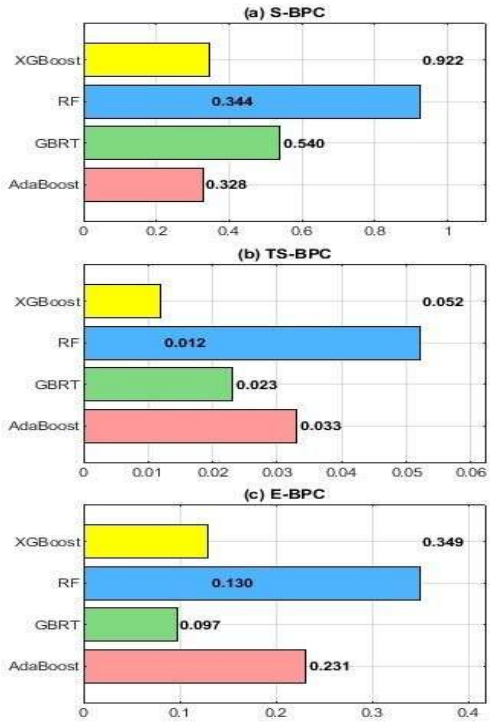

Fig. 13. Comparative summary of error metrics: RMSE), MAE, and OBJ, across FBIO-optimized models

For tensile strength prediction (TS-BPC), XGBoost–FBIO exhibited the most accurate results, achieving near-zero MAE values of 0.001 MPa (training) and 0.034 MPa (testing), alongside the lowest RMSE (0.003 MPa training, 0.031 MPa testing). This confirms its superiority in modeling tensile strength over other models, with GBRT–FBIO being a close second.

Regarding elastic modulus (E-BPC), GBRT–FBIO achieved the highest coefficient of determination values ($R^2 = 0.999$ in training and $R^2 = 0.974$ in testing) indicating excellent model fit. It also recorded the lowest RMSE and MAE values in both phases. Conversely, RF–FBIO consistently exhibited the weakest performance across all targets, with notably lower R^2 values (0.941 training, 0.880 testing for E-BPC) and higher error metrics.

To holistically assess model performance, the objective function (OBJ) was used as a composite metric incorporating multiple error indicators across training and testing datasets (Golafshani & Behnood, 2021). The GBRT–FBIO model achieved the lowest OBJ scores for E-BPC, underscoring its outstanding generalization and prediction quality. In contrast, RF–FBIO recorded the highest OBJ values for all three target properties (slump, tensile strength, and elastic modulus), reaffirming its comparatively lower reliability and predictive efficiency (Ashrafian et al., 2020).

In addition to standard evaluation metrics, two supplementary validation indicators were employed to assess model performance: the Scatter Index (SI) and the Nash–Sutcliffe Efficiency (NSE). The Scatter Index is a normalized metric that evaluates the dispersion of predicted values relative to observed data and is computed as the ratio of the Root Mean Square Error (RMSE) to the mean of observed values $\bar{Y}_{obs}$(*Sahoo et al.*, 2019). It is mathematically expressed as in formula (12).

$$SI = \frac{RMSE}{\bar{Y}_{obs}} \quad (12)$$

The Nash–Sutcliffe Efficiency (NSE) is a prominent statistical indicator commonly employed in hydrology, environmental science, and civil engineering to evaluate model accuracy. It assesses how well the predicted values replicate the variability observed in empirical data. An NSE score of 1 signifies an exact correspondence between model predictions and actual observations, whereas values near zero or negative reflect weak or inadequate model performance (McCuen et al., 2006). The mathematical expression for NSE is provided in Equation (13).

$$NSE = 1 - \frac{\sum_{i=1}^{N}(\mathrm{Y}_{pre} - \mathrm{Y}_{\mathrm{obs}})^2}{\sum_{i=1}^{N}(\mathrm{Y}_{obs} - \bar{\mathrm{Y}}_{\mathrm{obs}})^2} \quad (13)$$

The interpretation of the Nash–Sutcliffe Efficiency (NSE) and its complementary metric, the Scatter Index (SI), is based on established performance thresholds that categorize the predictive quality of a model. When the NSE value exceeds 0.75 or the SI value is below 0.1, the model is considered to have excellent predictive accuracy. A good level of performance is indicated when the NSE falls between 0.65 and 0.75, or the SI ranges from 0.1 to 0.2. Meanwhile, a fair level of prediction is assigned to models with NSE values between 0.5 and 0.65, or SI values from 0.2 to 0.318. These thresholds provide a practical framework for evaluating the reliability and precision of forecasting models in engineering and environmental applications.

As shown in Fig. 14, all FBIO-optimized models demonstrated strong predictive capability across the three concrete as evidenced by their Standard Index (SI) values. All SI scores remained below the 0.2 threshold, categorizing them as either "excellent" (SI < 0.1) or "good" (0.1 ≤ SI < 0.2) according to standard evaluation benchmarks. For S-BPC, the best performing models in the testing phase were XGBoost–FBIO (SI = 0.046) and AdaBoost–FBIO (SI = 0.066), indicating excellent predictive accuracy. In TS-BPC, both GBRT–FBIO and XGBoost–FBIO consistently achieved SI values below 0.1 for both training and testing, classifying them as excellent models. Meanwhile, for E-BPC, GBRT–FBIO again outperformed the others with testing SI = 0.128, reinforcing its superior generalization. In contrast, RF–FBIO exhibited the highest SI scores across all targets, particularly in the testing phase for E-BPC (SI = 0.342), placing it in the "fair" category and confirming its relatively weaker performance.

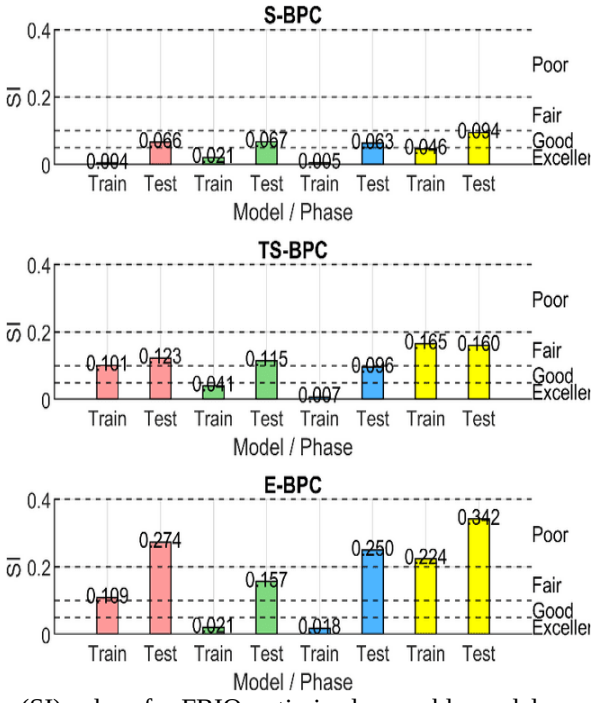

Fig. 14. Standard Index (SI) values for FBIO-optimized ensemble models across training and testing phases

The Taylor diagram as shown in Fig. 15. was employed to provide a comprehensive visual comparison of model performance by simultaneously illustrating three key statistical indicators:

standard deviation, root mean square error (RMSE), and the coefficient of determination (R^2). In this diagram, standard deviation is depicted as concentric circular contours centered on the origin, RMSE is shown by horizontal green markers indicating the deviation from observed values, and R^2 values are represented along a blue arc, reflecting the degree of correlation between predicted and observed data. Based on the Taylor plot, the GBRT-FBIO and XGB-FBIO models demonstrated superior performance compared to other approaches, consistently achieving better alignment with actual values across all evaluated properties.

The ensemble learning models particularly GBRT-FBIO for E-BPC and XGB-FBIO for S-BPC and TS-BPC demonstrated superior prediction capabilities, affirming findings from earlier studies (Amlashi et al., 2022). Their effectiveness in capturing nonlinear patterns and reducing prediction errors highlights the practicality of these hybrid ML frameworks for forecasting BPC performance efficiently.

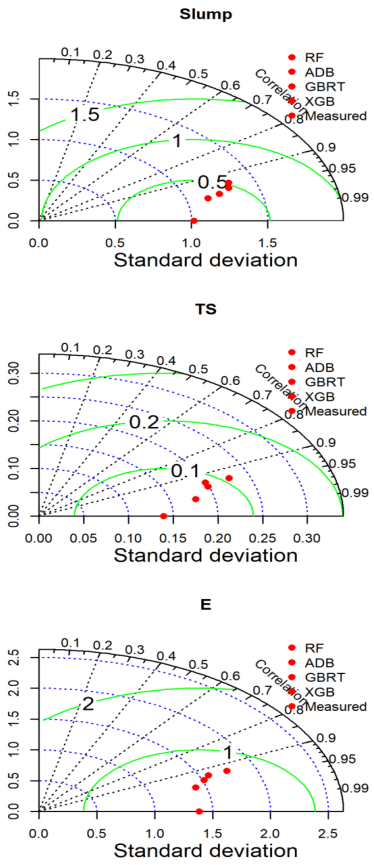

Fig. 15. Taylor diagrams comparing the performance of ensemble learning models against measured data for predicting.

The Nash–Sutcliffe Efficiency (NSE) presents values obtained during both training and testing phases for all FBIO-optimized models applied to S-BPC, TS-BPC, and E-BPC predictions. NSE is a widely recognized metric for evaluating the predictive accuracy of regression models, where values above 0.75 indicate excellent performance. All models exceeded this threshold across all targets and phases, confirming their high reliability.

For S-BPC, NSE values ranged from 0.990 (AdaBoost, training) to 0.920 (RF, testing), with all models achieving scores above 0.90 in both phases. Similarly, in the TS-BPC model, XGBoost achieved the highest NSE of 0.987 during training, followed by GBRT and AdaBoost, while even the lowest value (0.936 for RF in testing) remained well within the excellent range.

In the E-BPC scenario, GBRT and XGBoost maintained superior accuracy, reaching NSE values of 0.990 and 0.960 during training, respectively. The RF model again exhibited relatively lower performance, with a testing NSE of 0.866 the lowest among all models and targets yet still falling within the "good" to "excellent" classification.

The high NSE values across all predictions confirm the robustness and generalizability of the ensemble models, particularly XGBoost–FBIO and GBRT–FBIO, in modeling the mechanical behavior of bentonite plastic concrete (BPC).

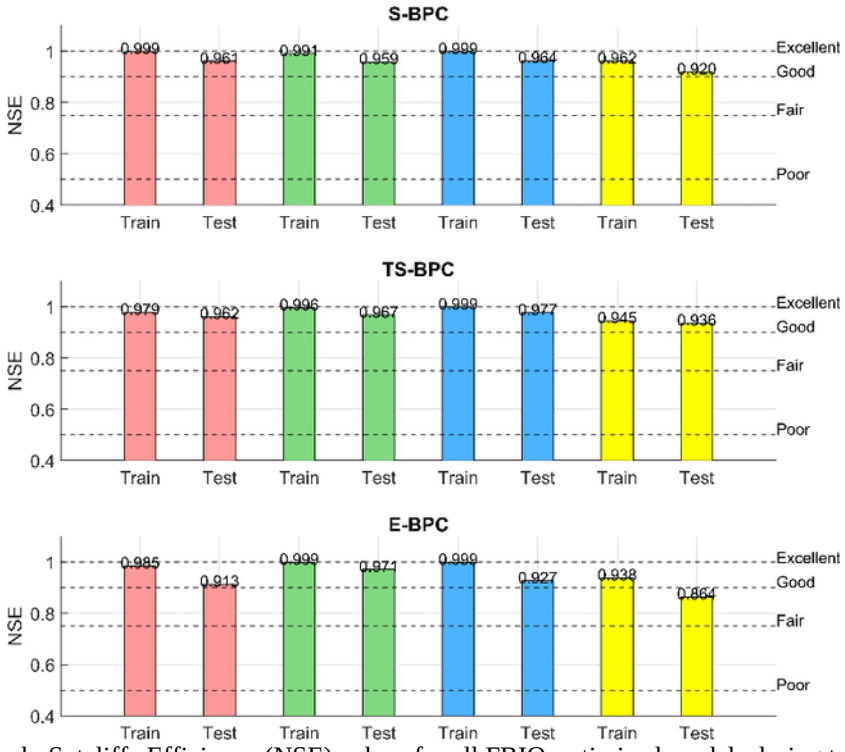

Fig. 16. Nash–Sutcliffe Efficiency (NSE) values for all FBIO-optimized models during training and testing phases across three target properties

4.2 Important Features Using SHAP Values

To improve the transparency of machine learning model predictions and better understand the influence of each input variable, this study applied SHapley Additive exPlanations (SHAP), a game-theoretic technique that quantifies the individual contribution of features to the output of predictive models (Lundberg & Lee, 2017). SHAP enhances interpretability by assigning each variable a specific value representing its marginal impact on the model's prediction. This method was implemented across the EL-FBIO to assess predictions related to S, TS, and EM in BPC.

The first stage of SHAP analysis involved evaluating average feature importance using bar plots of mean SHAP values as in Fig. 17. In the tensile strength model, cement and water were identified as the most influential features, highlighting their roles in hydration and mechanical performance. In the case of elastic modulus prediction, curing time and cement content demonstrated the most substantial influence, reflected by their average SHAP values of +0.18 and +0.12, respectively. These findings highlight their critical role in the evolution of concrete stiffness. Water and sand were identified as the most influential variables affecting workability, exhibiting average SHAP values of +0.11 and +0.09, respectively. Conversely, silty clay appearing in both the slump and elastic modulus models and bentonite predominantly in the tensile strength model showed negligible impact, indicating a limited sensitivity of the predicted outputs to fluctuations in their respective input values.

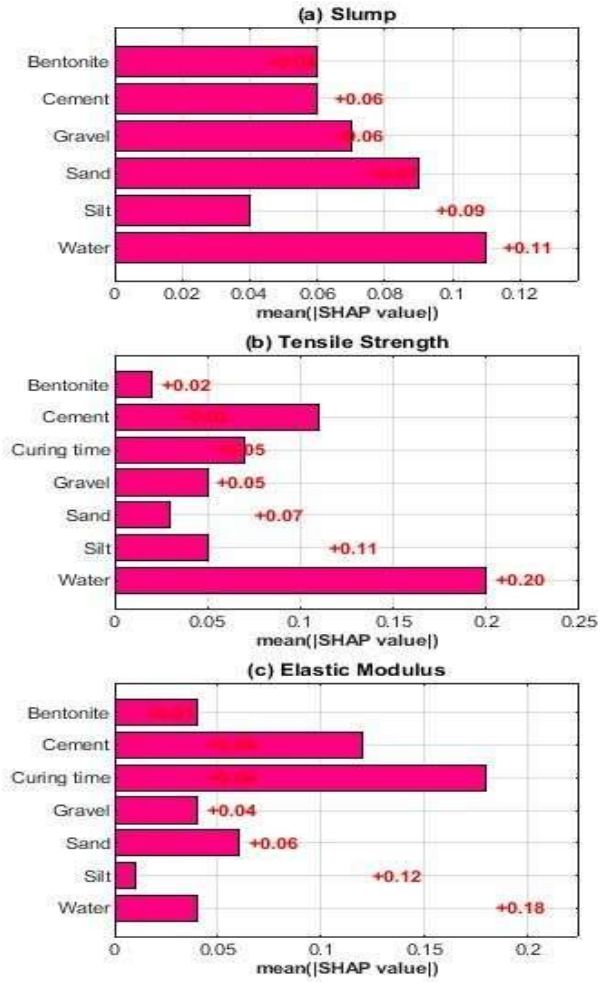

Fig. 17. Feature importance rankings for FBIO-optimized ensemble models across the three target properties

Further interpretability of the ensemble models was achieved through SHAP (SHapley Additive exPlanations) summary plots, as illustrated in Fig. 18. Each dot in these plots corresponds to a single prediction, with the horizontal axis representing the SHAP value which quantifies the contribution of each feature to the model output and the color gradient (blue to red) indicating the actual value of the feature from low to high. In the slump model (S-BPC), water content had the most substantial and consistent positive influence, as seen by its strong spread toward the positive SHAP range for high feature values. Conversely, bentonite and silt showed relatively narrow spreads, suggesting lower and more stable contributions to output variance.

In the tensile strength model (TS-BPC), curing time emerged as the most dominant feature, with high SHAP values and wide dispersion, highlighting its strong influence across different instances. Cement and gravel also exhibited moderate influence, while bentonite remained less impactful, consistent with its low SHAP dispersion.

For the elastic modulus model (E-BPC), curing time again demonstrated the broadest horizontal dispersion in SHAP values, affirming its critical role in governing stiffness. Cement content also had a significant positive contribution, especially at higher values, whereas bentonite displayed minimal SHAP variability, reinforcing its weak role in elastic behavior. Overall, these SHAP visualizations confirm that curing time and cement are the most influential predictors for mechanical properties in BPC, while bentonite contributes less consistently across all target variables.

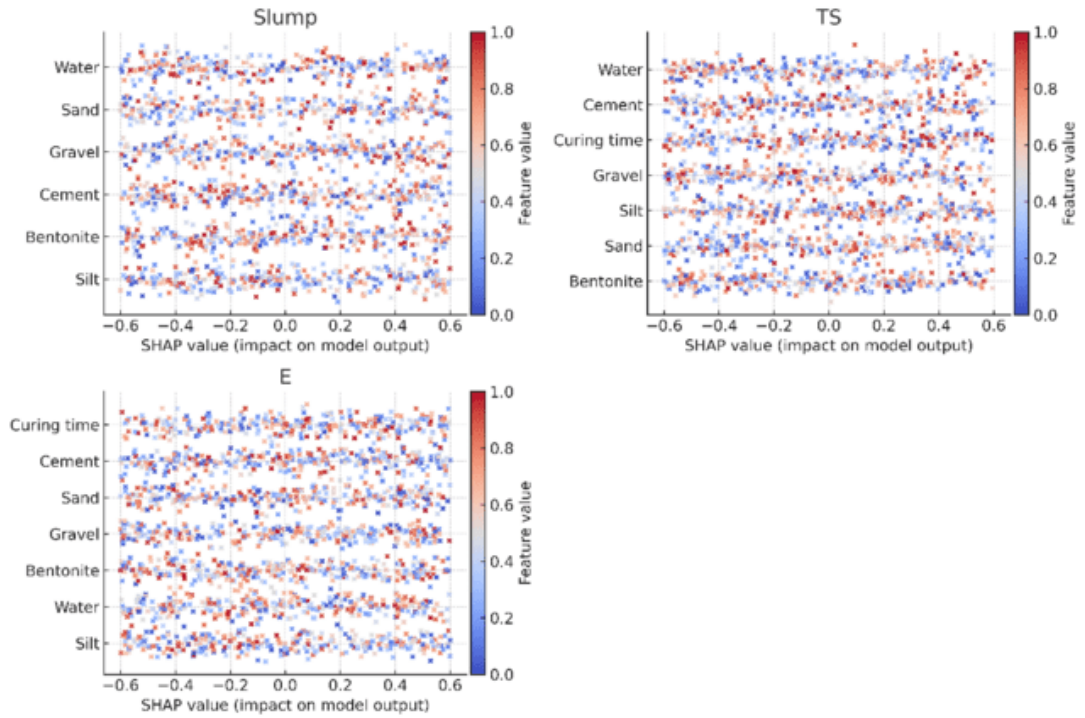

Fig. 18. SHAP summary plots for FBIO-optimized ensemble models predicting S-BPC, TS-BPC, and E-BPC.

The SHAP interpretability analysis revealed that cement and water-to-cement ratio were the most influential parameters, aligning with fundamental principles of concrete microstructure formation. High SHAP values for cement indicate its dominant role in strength gain, while negative SHAP values for excessive water-to-cement ratios confirm the weakening effect of increased porosity. Bentonite content showed a dual behavior improving cohesion at moderate levels but reducing strength at higher proportions due to excessive swelling. These interpretability insights provide practical guidance for optimizing BPC mix design, allowing engineers to balance workability, impermeability, and strength through data-informed proportioning.

To investigate the localized effects of input features on individual predictions, SHAP heatmaps were generated and are presented in Fig. 19. These visualizations depict the sample-wise variability in feature contributions for each target property. On the left, the fluctuation plots show the variation of predicted values across instances, while the heatmaps on the right illustrate SHAP value intensity and direction for each input parameter.

In the S-BPC model, water content emerged as the most influential feature, particularly for instances where predicted slump was below 15 cm. This is evident from the dominant red bands, indicating a strong positive SHAP contribution in those samples. Meanwhile, features like bentonite and silt maintained a relatively minor and uniform effect across all instances.

In the TS-BPC model, high tensile strength predictions consistently aligned with red SHAP values for water and curing time, highlighting their key roles in strength development. Notably, samples with lower predicted TS showed diminished SHAP intensity for these variables, suggesting their lesser impact in such cases.

For the E-BPC model, early-age predictions (left-hand side of the instance axis) showed intense red bands corresponding to curing time and cement, reflecting their substantial influence on early elastic modulus. These features gradually shifted to more balanced or cooler tones across later instances, indicating reduced dominance at higher ages or different mix conditions.

Overall, this heatmap-based SHAP analysis offers granular insight into how each feature dynamically contributes to the prediction outcomes across varying concrete samples, reinforcing the findings from global SHAP summaries.

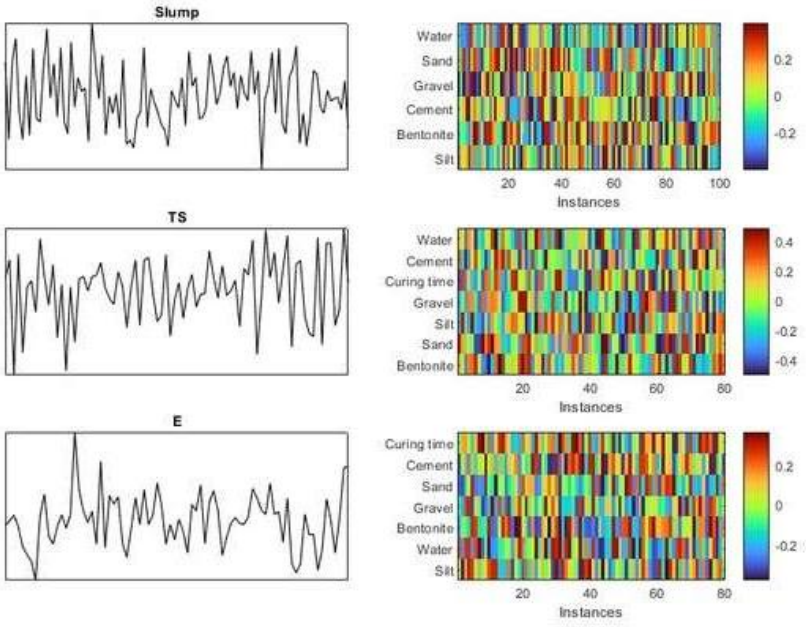

Fig. 19. SHAP heatmaps illustrating instance-level feature contributions for FBIO-optimized models

Previous studies have shown that machine learning models such as ANN, SVM, and MEP can effectively predict the mechanical properties of bentonite plastic concrete (BPC). For example, Khan et al. (2024) achieved very high correlation coefficients (R^2 = 0.9999 for slump, 0.9831 for compressive strength, and 0.9300 for elastic modulus) using the Multi-Expression Programming (MEP) model. Similarly, (Kumar et al., 2025) reported that the PSO-XGBoost model reached an R^2 of 0.974 and RMSE of 0.038, confirming the efficiency of metaheuristic-optimized boosting algorithms. (Huang et al., 2025) further demonstrated that optimization methods such as BOIvy can enhance prediction performance, while (Inqiad et al., 2024) highlighted water, cement, and bentonite as the most influential factors controlling BPC behavior.

In contrast, the present study extends these findings by developing an ensemble-based framework integrated with the FBIO algorithm. Unlike earlier studies that relied on single algorithms or manually tuned optimizers, this research applies four ensemble models (ADB, GBRT, XGB, and RF) automatically optimized through FBIO, eliminating parameter-setting complexity. The results revealed comparable or higher accuracy (R^2 up to 0.99 for tensile strength and 0.97 for elastic modulus) with improved model stability across multiple datasets. Moreover, SHAP analysis provided interpretable insights identifying curing time, cement, and water content as the dominant factors thereby bridging predictive performance with material understanding. Overall, this study demonstrates a more interpretable, efficient, and generalizable framework compared to previous ML-based BPC prediction approaches.

5. Limitations and Future Perspectives

While the proposed ensemble learning models, optimized via the Forensic-Based Investigation Optimization (FBIO) technique, demonstrated strong predictive capabilities across all evaluated mechanical properties of bentonite plastic concrete (BPC), several limitations remain. The primary constraint lies in the relatively limited size and diversity of the experimental datasets, which may affect the models' ability to generalize across broader construction scenarios.

Additionally, the reliance on secondary data sourced from previous studies may introduce inconsistencies due to variations in experimental protocols and measurement standards. Although SHAP analysis enhances interpretability, the inherent complexity of ensemble methods may still pose challenges for practitioners seeking intuitive understanding. The computational cost associated with FBIO, particularly in high-dimensional hyperparameter tuning, also presents a barrier to real-time deployment. Addressing these limitations through larger, more diverse

datasets, simplified model architectures, and alternative low-cost optimization methods will be essential for advancing the practical applicability and scalability of intelligent prediction systems in BPC engineering.

6. Conclusion

This study developed an interpretable and optimized ensemble learning framework integrated with Forensic-Based Investigation Optimization (FBIO) to predict the key mechanical properties of bentonite plastic concrete (BPC). Unlike conventional experimental or empirical methods, the proposed approach provides a data-driven alternative capable of delivering high predictive accuracy while reducing the need for time- and cost-intensive laboratory testing. By combining multiple ensemble algorithms (ADB, GBRT, XGB, and RF) with the adaptive FBIO optimizer, the framework achieves superior performance and computational efficiency compared to standalone models, establishing a novel optimization-based predictive paradigm for BPC analysis.

Beyond numerical performance, the integration of SHapley Additive exPlanations (SHAP) enabled a deeper understanding of how material constituents affect BPC behavior. Cement and curing time were identified as dominant contributors to strength and stiffness, while water-to-cement ratio and bentonite content exhibited nonlinear effects that govern workability and permeability. These interpretability insights translate directly into practical mix design guidance, offering engineers a transparent decision-support tool for optimizing sustainable and durable BPC formulations.

The research contributes to the broader field of sustainable materials engineering and digital transformation in construction by demonstrating how interpretable AI can bridge data science and material science for efficient design and environmental optimization. In doing so, it advances the application of machine learning in low-permeability and eco-efficient concretes, where conventional testing remains slow and resource-intensive.

Nevertheless, several limitations are acknowledged. The dataset, though comprehensive, may not fully represent large-scale field variability, and the computational demand of FBIO can increase with higher-dimensional datasets. Future studies should extend the framework to larger, multi-source datasets, incorporate environmental and curing conditions (e.g., temperature, humidity), and explore real-time predictive deployment in smart construction systems. Overall, the findings establish a replicable, interpretable, and sustainable AI-based pathway for performance prediction and optimization of BPC and related composite materials.

Acknowledgement

The authors would like to express their sincere gratitude to Universitas Muhammadiyah Yogyakarta for its invaluable support throughout the course of this research. The facilities, resources, and academic environment provided by the university played a vital role in the successful completion of this study. Although no external funding was received for this work, the institutional support from Universitas Muhammadiyah Yogyakarta is gratefully acknowledged.

References

Abbaslou, H., Ghanizadeh, A. R., & Amlashi, A. T. (2016). The compatibility of bentonite/sepiolite plastic concrete cut-off wall material. *Construction and Building Materials*, *124*. https://doi.org/10.1016/j.conbuildmat.2016.08.116

Albaijan, I., Fakhri, D., Hussein Mohammed, A., Mahmoodzadeh, A., Hashim Ibrahim, H., Babeker Elhag, A., & Rashidi, S. (2023). Several machine learning models to estimate the effect of an acid environment on the effective fracture toughness of normal and reinforced concrete. *Theoretical and Applied Fracture Mechanics*, *126*. https://doi.org/10.1016/j.tafmec.2023.103999

Alidoust, P., Goodarzi, S., Tavana Amlashi, A., & Sadowski, Ł. (2023). Comparative analysis of soft computing techniques in predicting the compressive and tensile strength of seashell containing concrete. *European Journal of Environmental and Civil Engineering*, *27*(5). https://doi.org/10.1080/19648189.2022.2102081

Al-Luhybi, A. S., & Qader, D. N. (2021). Mechanical Properties of Concrete with Recycled Plastic Waste. *Civil and Environmental Engineering*, *17*(2). https://doi.org/10.2478/cee-2021-0063

Alós Shepherd, D., & Dehn, F. (2023). Experimental Study into the Mechanical Properties of Plastic Concrete: Compressive Strength Development over Time, Tensile Strength and Elastic Modulus. *Case Studies in Construction Materials*, *19*. https://doi.org/10.1016/j.cscm.2023.e02521

Alyami, M., Nassar, R. U. D., Khan, M., Hammad, A. W., Alabduljabbar, H., Nawaz, R., Fawad, M., & Gamil, Y. (2024). Estimating compressive strength of concrete containing rice husk ash using interpretable machine learning-based models. *Case Studies in Construction Materials*, *20*. https://doi.org/10.1016/j.cscm.2024.e02901

Amlashi, A. T., Abdollahi, S. M., Goodarzi, S., & Ghanizadeh, A. R. (2019). Soft computing based formulations for slump, compressive strength, and elastic modulus of bentonite plastic concrete. *Journal of Cleaner Production*, *230*. https://doi.org/10.1016/j.jclepro.2019.05.168

Amlashi, A. T., Alidoust, P., Ghanizadeh, A. R., Khabiri, S., Pazhouhi, M., & Monabati, M. S. (2022). Application of computational intelligence and statistical approaches for auto-estimating the compressive strength of plastic concrete. *European Journal of Environmental and Civil Engineering*, *26*(8). https://doi.org/10.1080/19648189.2020.1803144

Ashrafian, A., Gandomi, A. H., Rezaie-Balf, M., & Emadi, M. (2020). An evolutionary approach to formulate the compressive strength of roller compacted concrete pavement. *Measurement: Journal of the International Measurement Confederation*, *152*. https://doi.org/10.1016/j.measurement.2019.107309

Bahrami, M., & Mir Mohammad Hosseini, S. M. (2022). A new incorporative element to modify plastic concrete mechanical characteristics for cut-off wall construction in very soft soil media: Identification of tensile galvanized open-mesh distributer (TGOD) element. *Construction and Building Materials*, *350*, 128884. https://doi.org/10.1016/J.CONBUILDMAT.2022.128884

Barakan, S., & Aghazadeh, V. (2021). The advantages of clay mineral modification methods for enhancing adsorption efficiency in wastewater treatment: a review. In *Environmental Science and Pollution Research* (Vol. 28, Issue 3). https://doi.org/10.1007/s11356-020-10985-9

Breiman, L., Friedman, J. H., Olshen, R. A., & Stone, C. J. (2017). Classification and regression trees. In *Classification and Regression Trees*. https://doi.org/10.1201/9781315139470

CAO, Y., MIAO, Q.-G., LIU, J.-C., & GAO, L. (2013). Advance and Prospects of AdaBoost Algorithm. *Acta Automatica Sinica*, *39*(6). https://doi.org/10.1016/s1874-1029(13)60052-x

Chen, T., & He, T. (2014). xgboost: Extreme Gradient Boosting. *R Lecture*, *2016*.

Chou, J. S., & Nguyen, N. M. (2020). FBI inspired meta-optimization. *Applied Soft Computing Journal*, *93*. https://doi.org/10.1016/j.asoc.2020.106339

Darimolyo, P. N., Zaki, A., & Riyadi, S. (2025). Prediction of natural frequency values in steel using multivariate regression. In M. T.I., P. S., A. E.A.M., A. B.C.R., A. C., S. D.M., H. A., & S. M.I. (Eds.), *AIP Conference Proceedings* (Vol. 3317, Issue 1). American Institute of Physics. https://doi.org/10.1063/5.0280774

de Myttenaere, A., Golden, B., Le Grand, B., & Rossi, F. (2016). Mean Absolute Percentage Error for regression models. *Neurocomputing*, *192*. https://doi.org/10.1016/j.neucom.2015.12.114

Deng, A. A. N., Ikhsan, J., Riyadi, S., & Zaki, A. (2024). Intelligent Forecasting of Flooding Intensity Using Machine Learning. *Civil Engineering Journal (Iran)*, *10*(10), 3269–3291. https://doi.org/10.28991/CEJ-2024-010-10-010

Dhar, A. K., Himu, H. A., Bhattacharjee, M., Mostufa, M. G., & Parvin, F. (2023). Insights on applications of bentonite clays for the removal of dyes and heavy metals from wastewater: a review. In *Environmental Science and Pollution Research* (Vol. 30, Issue 3). https://doi.org/10.1007/s11356-022-24277-x

Eftekhar Afzali, S. A., Shayanfar, M. A., Ghanooni-Bagha, M., Golafshani, E., & Ngo, T. (2024). The use of machine learning techniques to investigate the properties of metakaolin-based geopolymer concrete. *Journal of Cleaner Production*, *446*. https://doi.org/10.1016/j.jclepro.2024.141305

Ekanayake, I. U., Meddage, D. P. P., & Rathnayake, U. (2022). A novel approach to explain the black-box nature of machine learning in compressive strength predictions of concrete using Shapley additive explanations (SHAP). *Case Studies in Construction Materials*, *16*. https://doi.org/10.1016/j.cscm.2022.e01059

Elwell, D. J., & Fu, G. (1995). Compression testing of concrete: cylinders vs. cube. In *Special Report 119*.

Faraj, R. H., Hama Ali, H. F., Sherwani, A. F. H., Hassan, B. R., & Karim, H. (2020). Use of recycled plastic in self-compacting concrete: A comprehensive review on fresh and mechanical properties. In *Journal of Building Engineering* (Vol. 30). https://doi.org/10.1016/j.jobe.2020.101283

Fuqaha, S., Nugroho, G., & Zaki, A. (2025). Interpretable AI-Based Prediction of Elastic Modulus in Bamboo- Reinforced Polypropylene Using Mori – Tanaka and Neural Networks. *Diyala Journal of Engineering Sciences*, *8716*(3), 104–123. https://doi.org/10.24237/djes.2025.18307

Fuqaha, S., Zaki, A., & Nugroho, G. (2025). Machine learning and RSM for Strength Forecasting in Sustainable SCGC. *IIUM Engineering Journal*, *26*(3), 53–88. https://doi.org/https://doi.org/10.31436/iiumej.v26i3.3730

Gamil, Y. (2023). Machine learning in concrete technology: A review of current researches, trends, and applications. In *Frontiers in Built Environment* (Vol. 9). https://doi.org/10.3389/fbuil.2023.1145591

Ghanizadeh, A. R., Abbaslou, H., Amlashi, A. T., & Alidoust, P. (2019). Modeling of bentonite/sepiolite plastic concrete compressive strength using artificial neural network and support vector machine. *Frontiers of Structural and Civil Engineering*, *13*(1). https://doi.org/10.1007/s11709-018-0489-z

Golafshani, E. M., & Behnood, A. (2021). Predicting the mechanical properties of sustainable concrete containing waste foundry sand using multi-objective ANN approach. *Construction and Building Materials*, *291*. https://doi.org/10.1016/j.conbuildmat.2021.123314

Guan, Q., & Zhang, P. (2011). Effect of clay dosage on mechanical properties of plastic concrete. *Advanced Materials Research*, *250–253*. https://doi.org/10.4028/www.scientific.net/AMR.250-253.664

Hameed, R., Gul, M. M., Tahir, M., Shahzad, S., Jamil, O., Awais, M., & Asghar, Z. (2023). Mechanical Properties of Plastic Concrete Made Using Recycled Aggregates for Paving Blocks. *International Journal of Engineering Research in Africa*, *63*. https://doi.org/10.4028/p-hmjs0o

Hoang, N. D. (2022). Machine Learning-Based Estimation of the Compressive Strength of Self-Compacting Concrete: A Multi-Dataset Study. *Mathematics*, *10*(20). https://doi.org/10.3390/math10203771

Hu, L., Gao, D., Li, Y., & Song, S. (2012). Analysis of the influence of long curing age on the compressive strength of plastic concrete. *Advanced Materials Research*, *382*. https://doi.org/10.4028/www.scientific.net/AMR.382.200

Hu, L. M., Lv, X. L., Gao, D. Y., Yan, K. B., & Song, S. Q. (2014). Analysis of the influence of clay dosage and curing age on the strength of plastic concrete. *Advanced Materials Research*, *936*. https://doi.org/10.4028/www.scientific.net/AMR.936.1433

Huang, S., Li, C., Zhou, J., Mei, X., & Zhang, J. (2025). Use of BOIvy Optimization Algorithm-Based Machine Learning Models in Predicting the Compressive Strength of Bentonite Plastic Concrete. *Materials*, *18*(13). https://doi.org/10.3390/ma18133123

Iftikhar, B., Alih, S. C., Vafaei, M., Elkotb, M. A., Shutaywi, M., Javed, M. F., Deebani, W., Khan, M. I., & Aslam, F. (2022). Predictive modeling of compressive strength of sustainable rice husk ash concrete: Ensemble learner optimization and comparison. *Journal of Cleaner Production*, *348*. https://doi.org/10.1016/j.jclepro.2022.131285

Inqiad, W. B., Javed, M. F., Onyelowe, K., Siddique, M. S., Asif, U., Alkhattabi, L., & Aslam, F. (2024). Soft computing models for prediction of bentonite plastic concrete strength. *Scientific Reports*, *14*(1). https://doi.org/10.1038/s41598-024-69271-0

Iqbal, M. F., Liu, Q. feng, Azim, I., Zhu, X., Yang, J., Javed, M. F., & Rauf, M. (2020). Prediction of mechanical properties of green concrete incorporating waste foundry sand based on gene expression programming. *Journal of Hazardous Materials*, *384*. https://doi.org/10.1016/j.jhazmat.2019.121322

Karunasingha, D. S. K. (2022). Root mean square error or mean absolute error? Use their ratio as well. *Information Sciences*, *585*. https://doi.org/10.1016/j.ins.2021.11.036

Keramati, M., Goodarzi, S., Moradi Moghadam, H., & Ramesh, A. (2019). Evaluating the stress–strain behavior of MSW with landfill aging. *International Journal of Environmental Science and Technology*, *16*(11). https://doi.org/10.1007/s13762-018-2106-z

Khan, M., Ali, M., Najeh, T., & Gamil, Y. (2024). Computational prediction of workability and mechanical properties of bentonite plastic concrete using multi-expression programming. *Scientific Reports*, *14*(1). https://doi.org/10.1038/s41598-024-56088-0

Kibrete, F., Trzepieciński, T., Gebremedhen, H. S., & Woldemichael, D. E. (2023). Artificial Intelligence in Predicting Mechanical Properties of Composite Materials. *Journal of Composites Science*, *7*(9). https://doi.org/10.3390/jcs7090364

Kumar, P., Shekhar Kamal, S., Kumar, A., Kumar, N., & Kumar, S. (2025). Compressive strength of bentonite concrete using state-of-the-art optimised XGBoost models. *Nondestructive Testing and Evaluation*, *40*(10), 4868–4891. https://doi.org/10.1080/10589759.2024.2431634

Lal Mohiddin, S., Ravi Prasad, D., & Ramaseshu, D. (2025). A review of machine learning models for concrete strength prediction and mix optimization. *Journal of Building Pathology and Rehabilitation*, *10*(2). https://doi.org/10.1007/s41024-025-00636-2

Li, F., Rana, M. S., & Qurashi, M. A. (2025). Advanced machine learning techniques for predicting concrete mechanical properties: a comprehensive review of models and methodologies. *Multiscale and Multidisciplinary Modeling, Experiments and Design*, *8*(1). https://doi.org/10.1007/s41939-024-00672-4

Liu, Q., Zhou, Y., Lu, J., & Zhou, Y. (2020). Novel cyclodextrin-based adsorbents for removing pollutants from wastewater: A critical review. In *Chemosphere* (Vol. 241). https://doi.org/10.1016/j.chemosphere.2019.125043

Lundberg, S. M., & Lee, S. I. (2017). A unified approach to interpreting model predictions. *Advances in Neural Information Processing Systems*, *2017-December*.

Ly, H. B., Nguyen, M. H., & Pham, B. T. (2021). Metaheuristic optimization of Levenberg–Marquardt-based artificial neural network using particle swarm optimization for prediction of foamed concrete compressive strength. *Neural Computing and Applications*, *33*(24). https://doi.org/10.1007/s00521-021-06321-y

Mahboubi, A., & Ajorloo, A. (2005). Experimental study of the mechanical behavior of plastic concrete in triaxial compression. *Cement and Concrete Research*, *35*(2). https://doi.org/10.1016/j.cemconres.2004.09.011

McCuen, R. H., Knight, Z., & Cutter, A. G. (2006). Evaluation of the Nash–Sutcliffe Efficiency Index. *Journal of Hydrologic Engineering*, *11*(6). https://doi.org/10.1061/(asce)1084-0699(2006)11:6(597)

Moghaddam, H. M., Fahimifar, A., Ebadi, T., Keramati, M., & Siddiqua, S. (2025). Assessment of leachate-contaminated clays using experimental and artificial methods. *Journal of Rock Mechanics and Geotechnical Engineering*, *17*(1), 524–538. https://doi.org/10.1016/J.JRMGE.2024.02.050

Mousavi, S. M., Aminian, P., Gandomi, A. H., Alavi, A. H., & Bolandi, H. (2012). A new predictive model for compressive strength of HPC using gene expression programming. *Advances in Engineering Software*, *45*(1). https://doi.org/10.1016/j.advengsoft.2011.09.014

Nafees, A., Althoey, F., khan, S., Sikandar, M. A., Alyami, S. H., Rehman, M. F., Javed, M. F., & Eldin, S. M. (2023). Plastic concrete mechanical properties prediction based on

experimental data. *Case Studies in Construction Materials*, *18*. https://doi.org/10.1016/j.cscm.2023.e01831

Ni, B., Guo, S., Zhu, D., & Rahman, M. Z. (2025). A review on properties and multi-objective performance predictions of concrete based on machine learning models. *Materials Today Communications*, *44*. https://doi.org/10.1016/j.mtcomm.2025.112017

Nurega, B. A., Zaki, A., & Riyadi, S. (2025). Machine learning method to predict the compressive strength of cement mortar using a regression learner. In N. T., S. H., B. C., & M. I. (Eds.), *AIP Conference Proceedings* (Vol. 3320, Issue 1). American Institute of Physics. https://doi.org/10.1063/5.0286909

Pisheh, Y. P., & Mir Mohammad Hosseini, S. M. (2012). Stress-strain behavior of plastic concrete using monotonic triaxial compression tests. *Journal of Central South University of Technology (English Edition)*, *19*(4). https://doi.org/10.1007/s11771-012-1118-y

Qu, Z., Liu, H., Wang, Z., Xu, J., Zhang, P., & Zeng, H. (2021). A combined genetic optimization with AdaBoost ensemble model for anomaly detection in buildings electricity consumption. *Energy and Buildings*, *248*. https://doi.org/10.1016/j.enbuild.2021.111193

Ramezani, M., Choe, D.-E., & Rasheed, A. (2025). Prediction of the flexural strength and elastic modulus of cementitious materials reinforced with carbon nanotubes: An approach with artificial intelligence. *Engineering Applications of Artificial Intelligence*, *150*. https://doi.org/10.1016/j.engappai.2025.110544

Rathakrishnan, V., Bt. Beddu, S., & Ahmed, A. N. (2022). Predicting compressive strength of high-performance concrete with high volume ground granulated blast-furnace slag replacement using boosting machine learning algorithms. *Scientific Reports*, *12*(1). https://doi.org/10.1038/s41598-022-12890-2

Rozzaq, M. F. H., Zaki, A., & Riyadi, S. (2025). Predicting compressive strength of concrete with different grade using adaptive neuro fuzzy inference system. In M. T.I., P. S., A. E.A.M., A. B.C.R., A. C., S. D.M., H. A., & S. M.I. (Eds.), *AIP Conference Proceedings* (Vol. 3317, Issue 1). American Institute of Physics. https://doi.org/10.1063/5.0279547

Safavian, S. R., & Landgrebe, D. (1991). A Survey of Decision Tree Classifier Methodology. *IEEE Transactions on Systems, Man and Cybernetics*, *21*(3). https://doi.org/10.1109/21.97458

Sahoo, B. B., Jha, R., Singh, A., & Kumar, D. (2019). Application of Support Vector Regression for Modeling Low Flow Time Series. *KSCE Journal of Civil Engineering*, *23*(2). https://doi.org/10.1007/s12205-018-0128-1

Schapire, R. E. (1990). The strength of weak learnability. *Machine Learning*, *5*(2). https://doi.org/10.1007/bf00116037

Schapire, R. E. (2009). A Short Introduction to Boosting. *Society*, *14*(5). https://doi.org/10.1.1.112.5912

Shubber, M. D. H., & Kebria, D. Y. (2023). Thermal Recycling of Bentonite Waste as a Novel and a Low-Cost Adsorbent for Heavy Metals Removal. *Journal of Ecological Engineering*, *24*(5). https://doi.org/10.12911/22998993/161805

Svetnik, V., Liaw, A., Tong, C., Christopher Culberson, J., Sheridan, R. P., & Feuston, B. P. (2003). Random Forest: A Classification and Regression Tool for Compound Classification and QSAR Modeling. *Journal of Chemical Information and Computer Sciences*, *43*(6). https://doi.org/10.1021/ci034160g

Tavana Amlashi, A., Ghanizadeh, A., Abbaslou, H., & Alidoust, P. (2020). AUT Journal of Civil Engineering Developing three hybrid machine learning algorithms for predicting the mechanical properties of plastic concrete samples with different geometries. *Civil Eng*, *4*(1).

Tavana Amlashi, A., Mohammadi Golafshani, E., Ebrahimi, S. A., & Behnood, A. (2023). Estimation of the compressive strength of green concretes containing rice husk ash: a comparison of different machine learning approaches. *European Journal of Environmental and Civil Engineering*, *27*(2). https://doi.org/10.1080/19648189.2022.2068657

Turney, S. (2022). Coefficient of determination (R2): Calculation and interpretation. Scribbr.

Ullah, A., Yang, Y., Ullah, W., Ayub, B., Alzlfawi, A., & Iqbal, I. (2025). Toward transparent AI: Predicting strength of fly ash foam composite concrete using explainable ML models. *Structural Concrete*. https://doi.org/10.1002/suco.70302

Ullah, H. S., Khushnood, R. A., Farooq, F., Ahmad, J., Vatin, N. I., & Ewais, D. Y. Z. (2022). Prediction of Compressive Strength of Sustainable Foam Concrete Using Individual and Ensemble Machine Learning Approaches. *Materials*, *15*(9). https://doi.org/10.3390/ma15093166

Wu, H., Liu, C., Shi, S., & Chen, K. (2020). Experimental research on the physical and mechanical properties of concrete with recycled plastic aggregates. *Journal of Renewable Materials*, *8*(7). https://doi.org/10.32604/jrm.2020.09589

Xu, H., Zhou, J., Asteris, P. G., Armaghani, D. J., & Tahir, M. M. (2019). Supervised machine learning techniques to the prediction of tunnel boring machine penetration rate. *Applied Sciences (Switzerland)*, *9*(18). https://doi.org/10.3390/app9183715

Yang, H., Liu, X., & Song, K. (2022). A novel gradient boosting regression tree technique optimized by improved sparrow search algorithm for predicting TBM penetration rate. *Arabian Journal of Geosciences*, *15*(6). https://doi.org/10.1007/s12517-022-09665-4

Yang, Y., Liu, G., Zhang, H., Zhang, Y., & Yang, X. (2024). Predicting the Compressive Strength of Environmentally Friendly Concrete Using Multiple Machine Learning Algorithms. *Buildings*, *14*(1). https://doi.org/10.3390/buildings14010190

Zeng, Z., Zhu, Z., Yao, W., Wang, Z., Wang, C., Wei, Y., Wei, Z., & Guan, X. (2022). Accurate prediction of concrete compressive strength based on explainable features using deep learning. *Construction and Building Materials*, *329*. https://doi.org/10.1016/j.conbuildmat.2022.127082

Zhang, J., Wang, R., Lu, Y., & Huang, J. (2024). Prediction of Compressive Strength of Geopolymer Concrete Landscape Design: Application of the Novel Hybrid RF–GWO–XGBoost Algorithm. *Buildings*, *14*(3). https://doi.org/10.3390/buildings14030591

Zhang, M., & Kang, R. (2025). Machine learning methods for predicting the durability of concrete materials: A review. *Advances in Cement Research*. https://doi.org/10.1680/jadcr.24.00133

Zhang, P., Guan, Q., & Li, Q. (2013). Mechanical properties of plastic concrete containing bentonite. *Research Journal of Applied Sciences, Engineering and Technology*, *5*(4). https://doi.org/10.19026/rjaset.5.4867

Zhou, Z. H. (2012). Ensemble methods: Foundations and algorithms. In *Ensemble Methods: Foundations and Algorithms*. https://doi.org/10.1201/b12207